Extension of a static into a semi-dynamic traffic assignment model with strict capacity constraints

Brederode, Luuk; Gerards, Lotte; Wismans, Luc; Pel, Adam; Hoogendoorn, Serge

DOI
10.1080/23249935.2023.2249118

Publication date
2023

Document Version
Final published version

Published in
Transportmetrica A: Transport Science

Taylor & Francis
Taylor & Francis Group

Transportmetrica A: Transport Science

ISSN: (Print) (Online) Journal homepage: https://www.tandfonline.com/loi/ttra21

Extension of a static into a semi-dynamic traffic assignment model with strict capacity constraints

Luuk Brederode, Lotte Gerards, Luc Wismans, Adam Pel & Serge Hoogendoorn

To cite this article: Luuk Brederode, Lotte Gerards, Luc Wismans, Adam Pel & Serge Hoogendoorn (2023): Extension of a static into a semi-dynamic traffic assignment model with strict capacity constraints, Transportmetrica A: Transport Science, DOI: 10.1080/23249935.2023.2249118

To link to this article: https://doi.org/10.1080/23249935.2023.2249118

Published online: 24 Aug 2023.

TRANSPORTMETRICA A: TRANSPORT SCIENCE
https://doi.org/10.1080/23249935.2023.2249118

Taylor & Francis
Taylor & Francis Group

Extension of a static into a semi-dynamic traffic assignment model with strict capacity constraints

Luuk Brederode[a,b], Lotte Gerards[b], Luc Wismans[b,c], Adam Pel[a] and Serge Hoogendoorn[a]

[a]Department of Transport & Planning, Delft University of Technology, Delft, Netherlands; [b]DAT.mobility – a Goudappel Company, Deventer, Netherlands; [c]Centre for Transport Studies, Faculty of Engineering Technology, University of Twente, Enschede, Netherlands

ABSTRACT

To improve the accuracy of large-scale strategic transport models in congested conditions, this paper presents a straightforward extension of a static capacity-constrained traffic assignment model into a semi-dynamic version. The semi-dynamic model is more accurate than its static counterpart as it relaxes the empty network assumption, but, unlike its dynamic counterpart, maintains the stability and scalability properties required for application in large-scale strategic transport model systems. Applications show that, contrary to static models, semi-dynamic queue sizes and delays are very similar to dynamic outcomes, whereas only the congestion patterns differ due to the omission of spillback. The static and semi-dynamic models are able to reach user equilibrium conditions, whereas the dynamic model cannot. On a real-world transport model, the static model omits up to 76% of collective losses. It is therefore very likely that the empty network assumption influences (policy) decisions based on static model outcomes.

ARTICLE HISTORY
Received 30 December 2022
Accepted 11 August 2023

KEYWORDS
STAQ; semi-dynamic; traffic assignment model; user equilibrium; large-scale

1. Introduction

Strategic traffic assignment (TA) models are used to assess the long-term impact on route choices of transport policies and the design and management of transport systems. As road congestion has become a structural problem in ever more regions around the world, TA model accuracy in congested conditions has become more important.

Because strategic TA models are used for long-term forecasting, their outcomes should represent stable conditions in which travellers have adapted their route choice behaviour to the forecasted scenario. Stability conditions in TA models are mostly operationalised by imposing user equilibrium conditions (Wardrop 1952), where research suggests that a duality gap value (DG, the metric most used to measure the level of disequilibrium) of 1E-04 or lower is needed in strategic context (Boyce, Ralevic-Dekic, and Bar-Gera 2004; Brederode et al. 2019; Brederode, Heynicks, and Koopal 2016; Caliper 2010; Han et al. 2015; Patil,

CONTACT Luuk Brederode lbrederode@dat.nl Department of Transport & Planning, Delft University of Technology, Delft, Netherlands; DAT.mobility – a Goudappel Company, Deventer, Netherlands

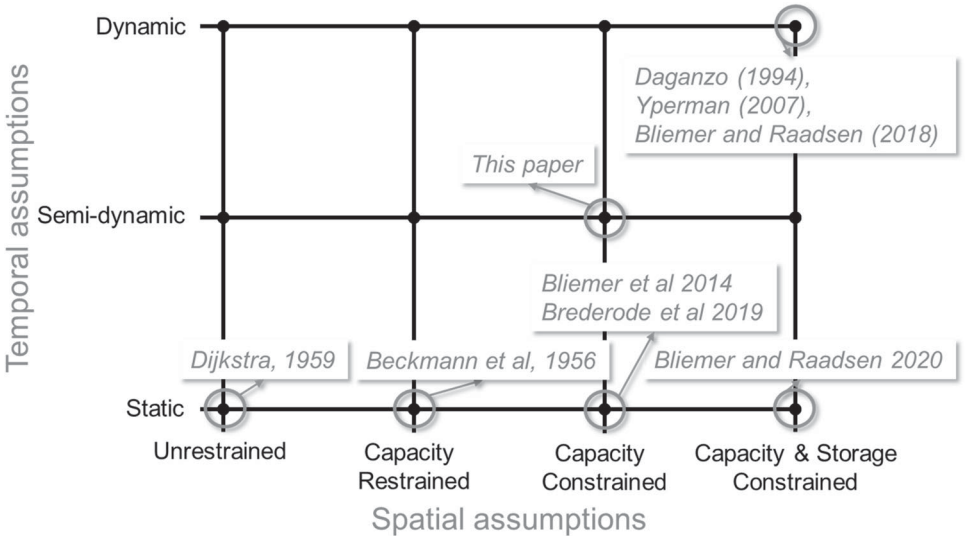

Figure 1. Simplified framework for classification of macroscopic TA model capabilities.

Ross, and Boyles 2021). Imposing equilibrium conditions on large-scale TA models involves iterative solution algorithms that are computationally expensive.

For strategic TA models, there is a clear trade-off between stability and computational requirements on the one hand and accuracy on the other hand (Bliemer et al. 2013; Brederode et al. 2019; Flötteröd and Flügel 2015). For each type of TA model, the trade-off is made differently. In this paper, the framework described in Bliemer et al. (2017) is used to define and classify the level of accuracy for different types of TA models. By only considering equilibrium models, the three-dimensional framework from Bliemer et al. (2017) simplifies into the two-dimensional framework depicted in Figure 1. In this framework, the accuracy of TA models is classified by their spatial and temporal assumptions, where static unrestrained TA models are the least accurate, while dynamic capacity and storage-constrained TA models are the most accurate. Below the effects of the different spatial and temporal assumptions on the accuracy of TA models are summarised, for a thorough description of the assumptions themselves the reader is referred to (Bliemer et al. 2017).

The spatial assumptions consider the effect of limited supply (capacity) on network usage and conditions. In unrestrained models (e.g.: All-Or-Nothing assignment), limited supply has no effect on the model outcome, whereas in capacity-restrained models (e.g. traditional static assignment models using BPR functions) route choice changes may occur due to limited supply although demand can still exceed supply. In capacity constrained models, route choice changes and vertical queues (and hence reduced flow downstream) may occur, whereas in capacity and storage-constrained models, route choice changes and horizontal queues (and hence spillback upstream and reduced flow downstream) may occur.

The temporal assumptions consider the effect that traffic that has departed but not arrived in previous time periods (residual traffic) has on network conditions (and hence usage) in the current time period. In static models, residual traffic has no influence on network conditions (i.e. the model assumes an empty network at the start of the considered

time period), whereas in semi-dynamic models residual traffic is transferred to the next time period (i.e. the model considers the residual traffic that is on the network at the start of each time period). In dynamic models, period durations are very small (causing almost all traffic to be residual traffic), and network conditions are updated on link (or even cell-) level, thereby implicitly 'transferring' traffic and network start conditions to the next time period.

1.1. Research goal, contributions, motivation, and paper outline

The goal of this research is to improve the accuracy of transport models in congested conditions whilst maintaining the stability and computational properties required for application in the strategic context. This paper builds upon Brederode et al. (2019) who demonstrated that shifting from (the still most widely used) static capacity restrained to a static capacity-constrained TA model indeed (greatly) improves model accuracy while satisfying the stability and computational requirements.

This paper investigates a further shift to the (even more accurate) semi-dynamic capacity-constrained TA model. By doing so, it contains two methodological contributions. Firstly, it extends the static capacity-constrained TA model described in Bliemer et al. (2014) and Brederode et al. (2019) to a semi-dynamic capacity-constrained TA model. Secondly, it derives expressions for collective loss and average delays from two perspectives (traveller's and network operator's) and three aggregation levels. Furthermore, it compares the proposed semi-dynamic TA model to its static and dynamic counterparts on theoretical networks as well as a large-scale realistic transport network. Further motivation for the choice of a semi-dynamic capacity-constrained TA model based on a literature review is given below.

For the last decades, emphasis has been mainly on the transition from *static* capacity-restrained TA models to *dynamic* capacity and storage-constrained TA models, where the most notable incarnations used in practice are the cell- (Daganzo 1994) and link- (Yperman 2007) transmission models. Although substantial progress for this model class has been made, both on computational efficiency (Bliemer and Raadsen 2018; Canudas-de-Wit and Ferrara 2018; Himpe, Corthout, and Tampère 2016; Himpe, Ginestou, and Tampère 2019; Petprakob et al. 2018; Simoni and Claudel 2020) as well as stability (Ge et al. 2020), as far as the authors are aware, there are still no examples where the stability requirement for strategic applications (duality gap values below 1E-04) is met.

More recently, research into *static* capacity and storage-constrained TA models show that these models also fail to meet the stability requirement (Bliemer and Raadsen 2020; Brederode et al. 2019; Smith 2013) whilst their computational requirements are not (yet) at acceptable levels for practitioners (Raadsen and Bliemer 2018). Hence, adding storage constraints to any model (either static or (semi-)dynamic) breaks convergence, which is in-line with theoretical findings (Han et al. 2015; Szeto and Lo 2006) that show that spillback can cause a non-continuous route cost function leading to non-convergence (Friesz and Han 2019). These findings are confirmed on multiple networks in Brederode et al. (2019) where on several large-scale networks a dynamic capacity and storage-constrained TA model assuming stationary demand did not converge below duality gap values below 1E-02 whereas a static capacity-constrained TA model on the same networks converged to duality gap values well below 1E-04.

Table 1. Semi-dynamic traffic assignment models in literature.

Publication	TA model type	Queues	Location and amount of residual traffic	Removal of flow downstream from bottleneck	User equilibrium type
Nakayama et al. 2012	Capacity restrained	None	Based on total travel time from speed flow function	No	Deterministic
Bui et al. 2019; Chan et al. 2021; Fusco, Colombaroni, and Sardo 2013; Koike, Nakayama, and Yamaguchi 2022; Nakayama and Connors 2014				Yes, as a post processing step to the TA model	Deterministic
Bell, Lam, and Lida 1996	Capacity constrained	Vertical at downstream end of bottleneck link	Based on location and size of vertical queues	No	Stochastic
Bell, Lam, and Lida 1996				No	Deterministic
Lam and Zhang 2000				Yes, part of assignment model	Deterministic
This paper		Vertical at node affected by capacity constraint(s)			Stochastic

As shown in Bliemer et al. (2014) and Brederode et al. (2019), static capacity constraint TA models already greatly improve accuracy in congested conditions compared to capacity-restrained TA models while maintaining scalability and stability properties required for strategic applications. Approaches using a semi-dynamic capacity restrained TA model (first two rows in Table 1) lack this accuracy improvement, as they omit modelling of queues. Instead, residual traffic is isolated by comparing the total travel time to the duration of the considered time period, assuming a uniform distribution of departure times. Most papers[1] (Bui et al. 2019; Chan et al. 2021; Fusco, Colombaroni, and Lo Sardo 2013; Koike, Nakayama, and Yamaguchi 2022; Nakayama and Connors 2014) also remove flow from links downstream from the location where the residual flow was transferred to the next time period, introducing an artificial feedback loop around the user equilibrium within each period itself reducing scalability and stability properties. Some approaches (e.g. Nakayama et al. 2012) therefore omit the removal of flow from downstream links altogether.

Given the above, to further increase accuracy without losing stability and/or low computational requirements, a shift from static capacity constrained towards a semi-dynamic capacity-constrained TA model seems to have the most potential.

Additionally, there are two application types for TA models that would benefit from a shift from a static to a semi-dynamic TA model. Firstly, because semi-dynamic TA models do not assume an empty network at the start of the assignment, they provide a much better application context to add departure time choice models to the transport model

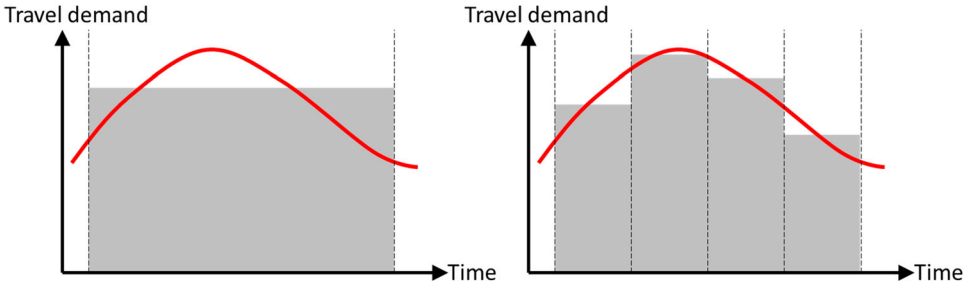

Figure 2. Left: single time period with stationary travel demand (static assumption) vs. right: multiple time periods with stationary demand (semi-dynamic assumption).

system than their static counterparts do. Secondly, in the context of demand matrix estimation, a semi-dynamic TA model allows to account for observed link flows that are partially composed of traffic that departed prior to the considered time period.

In conclusion, the semi-dynamic capacity-constrained TA model is selected because, contrary to capacity and storage-constrained TA models, it is expected to meet stability and computational requirements whilst it is expected to substantially improve accuracy compared to its static capacity-constrained and capacity-restrained counterparts, especially in the application contexts of departure time choice modelling and demand matrix estimation.

The remainder of this paper is organised as follows. Section 2 positions the proposed semi-dynamic capacity-constrained TA model in the field, whereas section 3 describes the algorithms used to solve it and to derive collective losses and average delays from its outcomes. In section 4, the accuracy, stability, and scalability properties of the model are evaluated using applications on two theoretical and one real-scale transport model instance. In section 5, properties and limitations specific to the semi-dynamic TA model are discussed. Finally, conclusions are drawn in section 6 along with recommendations for further research.

2. From static to semi-dynamic: relaxing the empty network assumption

To further position the semi-dynamic TA model subject of this paper, this section describes how it is derived from its static capacity-constrained counterpart described in (Bliemer et al. 2014) and compares it to semi-dynamic TA models in literature.

2.1. From a single to multiple time periods with stationary travel demand

To extend the static capacity-constrained TA model described in Bliemer et al. (2014) to the semi-dynamic capacity-constrained TA model used in this paper, the model assumption of a single time period with stationary travel demand is relaxed into the assumption that there are multiple time periods with stationary travel demand. This is illustrated in Figure 2, where some 'true' travel demand (red line) is converted to stationary travel demand for static (left) and semi-dynamic (right) TA models.

Other model properties and assumptions are maintained, most importantly: the node model from Tampère et al. (2011) and a fundamental diagram with a horizontal hypercritical branch (Figure 4, left) are used. With respect to flow propagation, instantaneous forward propagation of vehicles is assumed on uncongested links, whereas the horizontal hypercritical branch of the fundamental diagram implies backward wave speeds of zero and hence vertical queues.

The instantaneous forward propagation assumption means that all traffic that is not held up in queues by definition arrives at its destination within the duration of the considered time period. Strictly adhering to this assumption, the semi-dynamic TA model in this paper only transfers traffic held up in queues to the subsequent time period where it may re-evaluate its route choice. By doing so, the favourable scalability and stability properties of the static capacity-constrained TA model from Bliemer et al. (2014) are maintained.

To conclude: the relaxation from a single into multiple time periods in combination with the other (unchanged) model assumptions effectively means that it is no longer assumed that the network is empty at the start of each time period, but already contains traffic that was held up in queues in the previous time period.

2.2. Semi-dynamic traffic assignment in literature

Table 1 provides an overview of literature on semi-dynamic[2] traffic assignment models.

Contrary to approaches using a semi-dynamic capacity-restrained TA model (the first two rows in Table 1, already reviewed in subsection 1.1) approaches using a capacity-constrained TA model (the last four rows in Table 1) do model queues, and only transfer traffic that is held up in them to the next time period. To enforce capacity constraints, the TA models in Bell, Lam, and Lida (1996), Lam and Zhang (2000), and Lam, Lo, and Zhang (1996) employ exit link capacities, thereby assuming vertical queues on the downstream end of bottleneck links, whereas the TA model used in this paper (last row in Table 1) more accurately puts the vertical queue on the upstream end of the bottleneck link. Just like Nakayama et al. (2012), the approaches in Bell, Lam, and Lida (1996) and Lam, Lo, and Zhang (1996) omit the removal of queued flow from downstream links, whereas the approach in this paper as well as Lam and Zhang (2000) queued flow is removed from downstream links as part of the TA model itself.

3. Solution algorithm

To extend the static capacity-constrained TA model described in Bliemer et al. (2014) into a semi-dynamic version, our previous static capacity-constrained TA model implementation (Brederode et al. 2019) was not altered. Instead, as shown in Figure 3, it is set in a loop with a residual traffic transfer module and post-processing modules that update cumulative in- and out-flow curves and derive travel times from those curves are added. In the remainder of this section, the mathematical notation used to describe the solution algorithm is defined in the text. For the convenience of the reader, appendix A lists all indices, sets, constants, variables, and vectors.

Subsection 3.1 describes the static capacity-constrained TA model. It is applied for each time period $k \in K$ with end time t_k, yielding a set of inflows for all links $\mathbf{u}_k$, route choice probabilities ($\boldsymbol{\pi}_k$) for each route in the route set, and a set of flow acceptance factors $\boldsymbol{\alpha}_k$

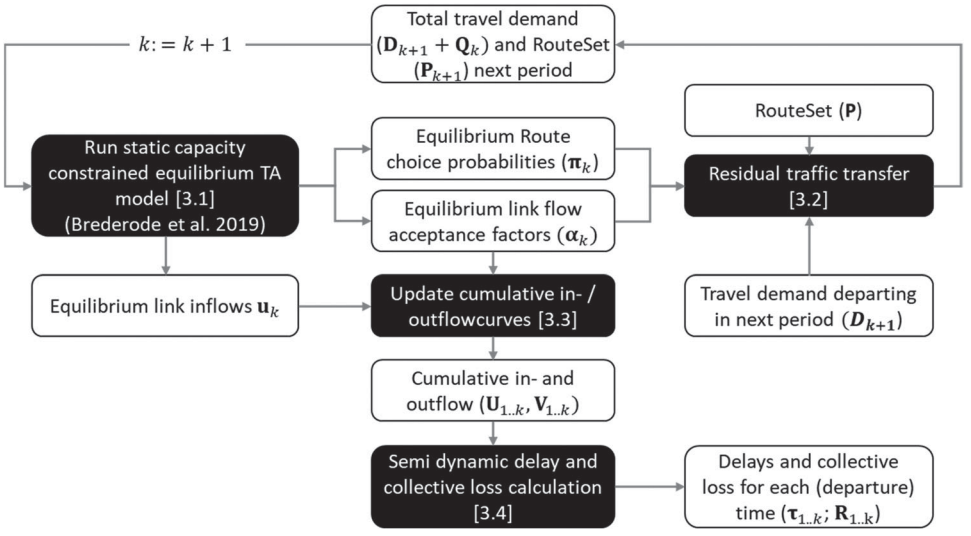

Figure 3. Overview of the proposed solution algorithm (subsection numbers between squared brackets).

(representing the proportion of flow that is not held up in a queue) for all links that have a vertical queue on its downstream node.

The residual traffic transfer module (subsection 3.2) uses the route choice probabilities and link flow acceptance factors to transfer flow that is held up in queues ($\mathbf{Q}_k$) to the travel demand matrix of the next time period and to update the route set to include routes from the location of vertical queues to the original destinations of routes traversing these queues.

Finally, modules that update cumulative in- and out-flow curves (subsection 3.3) and conduct delay calculations on link-, route- and network-level (subsection 3.4) are added to derive collective losses and average delays per (departure) time period from link inflows and flow acceptance factors. Note that the loop consisting of the static capacity-constrained TA model and residual traffic transfer together form the semi-dynamic TA model. Further note that the cumulative flow updating and delay calculation modules are optional post-process modules and that (repetitive) delay calculation on route level also takes place as part of the static capacity-constrained TA model using the delay formulation from Bliemer et al. (2014). The difference is that the delay calculation within the TA model (subsection 3.1) assumes an empty network after the current time period (hence, it uses 'static delays'), whereas the semi-dynamic delay calculation (subsection 3.4) takes traffic on the network in the next time period into account (hence it derives 'semi-dynamic delays').

3.1. Static capacity constrained TA model

The TA model STAQ described in Brederode et al. (2019) is the central module in the solution algorithm proposed in this paper. Several variations of the propagation model within STAQ are described in Brederode et al. (2019), varying with respect to the nature of queues (horizontal or vertical), the fundamental diagram (triangular or Quadratic-Linear), and the

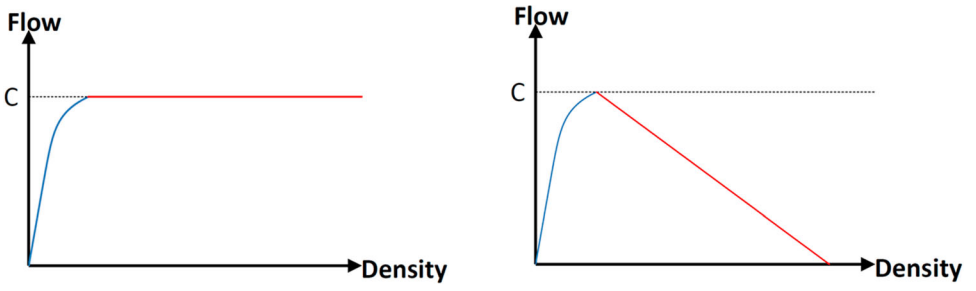

Figure 4. Left: quadratic-horizontal fundamental diagram (used while equilibrating route demands); right: quadratic-linear fundamental diagram (used while translating vertical equilibrium queues into horizontal queues).

inclusion of junction modelling (disabled, only turn delays or turn delays and turn flow restrictions).

The STAQ variation with vertical queues is used to converge towards the stochastic user equilibrium (SUE, Fisk 1980), after which a single iteration with horizontal queuing is conducted to translate equilibrium queues horizontally. The quadratic-linear fundamental diagram (Figure 4, right) is selected, which – while equilibrating based on vertical queues – simplifies to quadratic-horizontal fundamental diagram (Figure 4, left). With respect to junction modelling, both turn delays and turn flow restrictions are included.

A pre-generated route set **P** is used, derived from the digitised transport network combining the Dijkstra algorithm to find the shortest routes with the repeated random sampling process on free flow link travel times from Fiorenzo-Catalano (2007) to generate alternative routes. Route set filters are applied to reduce route overlap, remove irrelevant routes and restrict the size of the route set.

Route choices are modelled through the multinomial logit (MNL) model such that route choice probability $\pi_{p,rs}$ for route p on OD-pair rs is defined by:

$$\pi_{p,rs} = \exp(-\mu_{rs} c_p) / \sum_{p' \in P_{rs}} \exp(-\mu_{rs} c_{p'}) \tag{1}$$

where c_p represents the route cost on route p, μ_{rs} is the scale parameter describing the degree of travellers' perception errors on route travel cost and P_{rs} is the set of routes between r and s. Note that for brevity in this subsection the argument (k) is omitted from all variables, because within the static capacity-constrained TA model, there are no relationships with other time periods. Note that, without loss of generality, but at the cost of computational efficiency, the MNL route choice model could be replaced by more advanced route choice models (e.g. Prato 2009; Smits et al. 2018).

To enforce and speed up the equilibration of route demands, for non-theoretical test applications, the self-regulating average (Liu, He, and He 2007) is used to average route choice probabilities over iterations. To check for convergence to conditions of the stochastic user equilibrium conditions, the adapted relative duality gap as derived in Bliemer et al. (2013) is used, which accounts for perception errors and thus reaches zero upon

convergence when using the MNL route choice model:

$$DG = \frac{\sum_{rs \in RS} \sum_{p \in P_{rs}} \pi_{p,rs} D_{rs} (c_p + -\mu_{rs}^{-1} \ln(\pi_{p,rs} D_{rs} - \zeta_{rs})}{\sum_{rs \in RS} D_{rs} \zeta_{rs}} \tag{2}$$

where RS is the set of OD-pairs, D_{rs} is the demand on OD-pair rs, and $\zeta_{rs} = \min_{p \in P_{rs}} [c_p + \mu_{rs}^{-1} \ln \pi_{p,rs} D_{rs}]$ represents the minimum stochastic route cost on OD pair rs. In line with Boyce, Ralevic-Dekic, and Bar-Gera (2004), Brederode et al. (2019), Han et al. (2015) and Patil, Ross, and Boyles (2021), for non-theoretical test applications in this paper, a threshold value of 1E-04 is used as the stop criterion for the traffic assignment model.

Next to link inflows $\mathbf{u}$ and route choice probabilities $\boldsymbol{\pi}$, the TA model provides flow acceptance factors α_{ij} for each turning movement (turn) from inlink i to outlink j. Flow acceptance factors represent the proportion of flow that passes that turn, the remainder of flow using the turn (i.e. proportion $1 - \alpha_{ij}$) is left on the turn as a vertical queue. To ensure that all traffic reaches its destination according to the route definitions in $\mathbf{P}$ and route probabilities $\boldsymbol{\pi}$, the node model within STAQ assumes the first-in-first-out (FiFo) principle (Daganzo 1995), which in the context of STAQ means that flow acceptance factors for all turns sharing an inlink are equal, i.e. $\alpha_i = \alpha_{ij}$ for all outlinks j connected to the node considered.

3.2. Residual traffic transfer

The goal of the residual traffic transfer module is to transfer travel demand that was held up in queues in the TA model for period k to the travel demand matrix for period $k + 1$ such that it resumes its route from the location of the queue to its original destination.

The set of acceptance factors on turns with residual queues for period k is denoted by $\boldsymbol{\alpha}_k$. The acceptance factors are used together with the OD-demands $\mathbf{D}_k = \{D_{rs}(k) \forall rs \in RS\}$ and the route choice probabilities $\boldsymbol{\pi}_k = \{\pi_{p,rs}(k) \forall p \in P\}$ to calculate the amount of residual traffic $Q_{ij,s}(t_k)$ between turn ij and destination s using:

$$Q_{ij,s}(t_k) = (1 - \alpha_i(k)) \sum_{p \in P_{ij}} \pi_{p,rs}(k) D_{rs}(k) \prod_{i'j' \in IJ_{p,i}} \alpha_{i'}(k) \tag{3}$$

where P_{ij} represents the set of routes traversing considered turn ij and $IJ_{p,i}$ represents the set of turns on route p up to but excluding the turn from link i to link j. The first term in Equation (3), represents the proportion of demand that is held up in the queue on turn ij, whereas the second term represents the amount of demand that arrives at link i, taking reductions due to upstream queues into account.

The amount $Q_{ij,s}(t_k)$ of traffic is then transferred to the travel demand matrix of the next time period using a centroid connected to the upstream node of the link with the vertical queue as origin and the original destinations of the paths in P_{ij}. Furthermore, partial routes between this new centroid and the destinations of routes passing it are added to the route set.

Note that the centroid could also be directly connected to the node from which the vertical queue was transferred, allowing to steer the priority of the transferred demand over demand departed in the current period, by altering the capacity of the connector link. This idea will be further discussed in subsection 5.3, but for the sake of scalability and simplicity

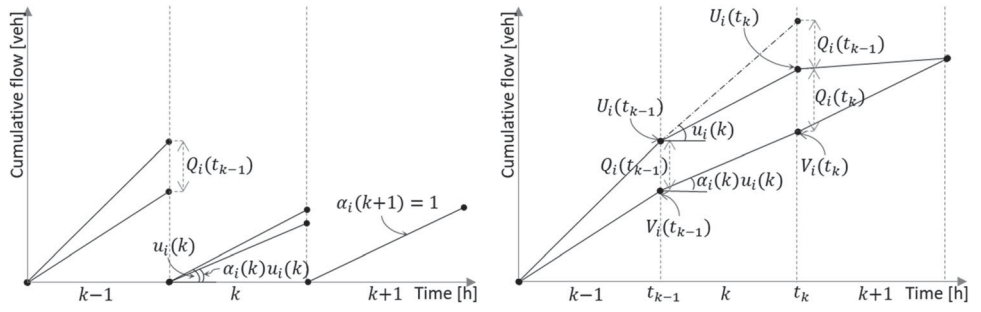

Figure 5. Example of consecutive static cumulative flow curves (left) and corresponding semi-dynamic cumulative flow curves (right) demonstrating much larger link travel times in the semi-dynamic case due to residual traffic transfer.

of the algorithm (it would require bookkeeping of transferred demand), its implementation and analysis are left for further research.

3.3. Updating cumulative in-/out-flow curves

After each time period, for each link *i* on which a vertical queue remains or has remained in previous time periods, static cumulative in- and outflow curves are constructed using the duration of the time period and the link inflows and acceptance factors from the assignment. As an illustrative example, Figure 5, left displays static cumulative in- and outflow curves of some fictitious link *i* for time periods [*k* - 1..*k* + 1]. In time periods *k* - 1 and *k*, the outflow curves are below the inflow curves, indicating that a vertical queue is present on the downstream end of the link. From these curves, the semi-dynamic piece-wise linear cumulative in- and out-flow curves (Figure 5, right) are constructed using:

$$\begin{aligned} U_i(t_k) &= U_i(t_{k-1}) + u_i(k)(t_k - t_{k-1}) - Q_i(t_{k-1}) \\ V_i(t_k) &= V_i(t_{k-1}) + \alpha_i(k)u_i(k)(t_k - t_{k-1}) \end{aligned} \tag{4}$$

where $U_i(t_k)$ and $V_i(t_k)$represent the cumulative inflow and outflow respectively for link *i* at the end of period *k*, and $u_i(k)$ represents the inflow rate of link *i* during period *k*. Note that to avoid double-counting, as illustrated by the dashed cumulative inflow curve in the right part of Figure 5, the residual traffic transferred on link *i* from the previous period, $Q_i(t_{k-1})$, is subtracted from the static cumulative inflow curve since $u_i(k)$ includes residual traffic transferred from period *k* - 1. For the interested reader, two expressions to derive $Q_i(\cdot)$ are shown in Appendix B.

As first described in Lo and Szeto (2002), horizontal distances between cumulative inflow and outflow curves represent the link travel time at a given point in time. Because STAQ assumes instantaneous forward flow propagation (subsection 2.1), here the distance between the cumulative inflow curve and the cumulative outflow curve represents the link delay instead of the travel time. Additionally, the stationary travel demand assumption in STAQ causes the cumulative flow curves to be piece wise linear with tipping points only occurring at the start time of the time periods defined for the semi-dynamic TA model, allowing for easy calculation of time-averaged delays by dividing the surface between

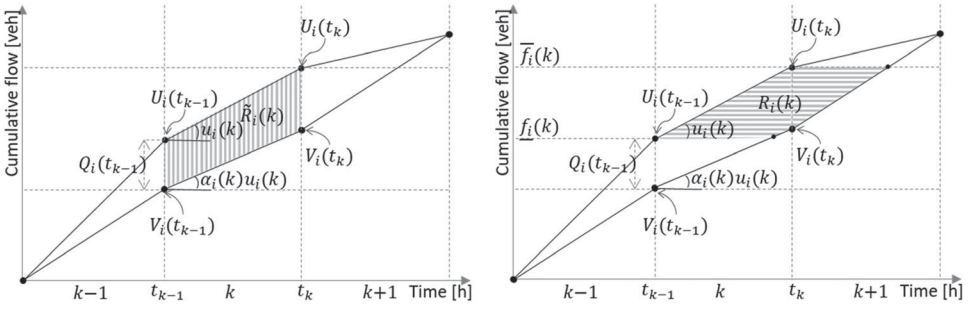

Figure 6. Example of cumulative link flow curves for three time periods. Left: shaded area represents the collective loss from the network operator's perspective. Right: shaded area represents the collective loss from the traveller's perspective (for a link that is not used by routes affected by upstream bottlenecks in time periods *k* - 1 and k).

the curves (representing collective losses) by the number of vehicles experiencing this collective loss.

3.4. Calculating collective loss and average delays

Collective travel time losses can be derived either from the perspective of the network operator or the traveller. From the network operator's perspective, $\widetilde{R}_i(k)$ represents the collective time loss of vehicles *using* link *i* during period *k* (shaded area in Figure 6, left), whereas from the traveller's perspective $R_i(k)$ represents the collective time loss of vehicles using link *i* that have *departed* (or resumed as residual traffic from a queue) during period *k* (shaded area in Figure 6, right). Interpretation of the differences between the shaded areas in Figure 6 shows that the loss from traveller's perspective is equal to the loss from operator's perspective minus the loss experienced in the current period by travellers that departed in the previous period (the triangle bounded by $Q_i(t_{k-1})$, $\underline{f}_i(k)$ and $V_i(\cdot)$) plus the loss experienced in the next period by travellers that departed in the current period (the triangle bounded by t_k, $\overline{f}_i(k)$ and $V_i(\cdot)$).

Which of the perspectives is most appropriate depends on the application type. Table 2 summarises typical application types for collective time loss and average delay calculation for both perspectives and for different levels of aggregation (link-, route- and network-level).

3.4.1. Network operator's perspective

On the link level, a typical application type for the network operator's perspective is to determine which links and during which time periods collective losses occur. Illustrated in the right part of Figure 6, the surface representing the collective loss in the network operator's perspective may be calculated using simple geometry:

$$\tilde{R}_i(k) = \frac{(t_k - t_{k-1})(U_i(t_{k-1}) - V_i(t_{k-1}) + U_i(t_k) - V_i(t_k))}{2} \tag{5}$$

where $\tilde{R}_i(k)$ represents the collective loss of traffic on link *i* during period *k*. Average delay is derived by dividing collective loss by the number of vehicles using the link during

Table 2. Application types for travel time calculation per aggregation level for network operator's and traveller's perspectives.

	Collective loss / average delay experienced by vehicles …	
	… on the network within a given time period Network operator's perspective	… departed within a given time period Traveller's perspective
Link-level	• Application type: To determine where and when collective loss occurs • Collective loss on link i during period k: $\tilde{R}_i(k)$ – Equation (5) • Average delay per vehicle on link i during period k: $\tilde{\tau}_i(k)$ – Equation (6)	• Application type: To derive the od-link incidence indicator within semi-dynamic matrix estimation • Collective loss of vehicles using link i departed during k: $R_i(k)$ – Equation (14) • Average delay per vehicle departed during period k on link i: $\tau_i(k)$ – Equation (17)
Route-level	• Not relevant from network operator's perspective, as for travellers, only the non-instantaneous travel time to complete a route is of importance.	• Application type 1: route cost calculation within the semi-dynamic user equilibrium; • Application type 2: to use in a departure time choice model; • Average delay per vehicle departed during period k using route p upto link i: ○ for application type 1: $\dot{\tau}_{p,i}(k)$ – Equation (19) ○ for application type 2: $\tau_{p,i}(k)$ – Equation (20)
Network-level	• Application type: To quantify network performance over time • Network wide collective loss during period k: $\tilde{R}(k)$ – Equation (7)	• Application type: To quantify network performance per departure time • Network wide collective loss for vehicles departed during period k: $R(k)$ – Equation (18)

period k:

$$\tilde{\tau}_i(k) = \frac{\tilde{R}_i(k)}{U_i(t_k) - V_i(t_{k-1})} \tag{6}$$

where $\tilde{\tau}_i(k)$ represents the average delay per vehicle on link i during period k.

On the network level, a typical application type from the network operator's perspective is to quantify network performance over time. This is done by simply summing all link-level collective losses:

$$\tilde{R}(k) = \sum_i \tilde{R}_i(k), \tag{7}$$

where $\tilde{R}(k)$ is the network-wide collective loss during period k.

Note that Equations (5) and (6) are the equivalent to the average delay function from the 'longitudinal semi-dynamic perspective' in Raadsen and Bliemer (2019), albeit that their formulation represents the average delay experienced by traffic *flowing out of* link i during time period k (it divides collective loss by the amount of traffic that has flown out), whereas our formulation for the network operator's perspective represents the average delay experienced by traffic *on link* i during time period k (Equation 6 divides collective loss by the amount of traffic that was on the link). Further note that on the route level, no application type for the network operator's perspective could be identified, so expressions for this aggregation level are omitted.

3.4.2. Traveller's perspective – link and network level

On the link level, a typical application type for the traveller's perspective is to derive the od-link incidence indicator within (semi-dynamic) matrix estimation on observed link travel times. To determine collective loss and average delays from the traveller's perspective, three steps are conducted. First, the range of cumulative flow that departed in the considered departure time period is derived. Then, the points in time on which the first and last vehicles entered and exited the considered link are calculated and added to the set of relevant points in time. Finally, the collective loss and link delays for traffic that departed in the considered time period are derived.

3.4.2.1. Calculation of cumulative flow levels of first and last vehicle departed in considered time period. For reasons of clarity, two types of links are distinguished when determining the cumulative flow range. The first type is links that in the previous time period were only used by traffic on routes unaffected by active bottleneck(s) upstream (i.e.: links that were only used by paths for which $\prod_{i'j' \in IJ_{p,i}} \alpha_{i'}(k) = 1$). Illustrated in the right part of Figure 6, for these links the cumulative flow that departed during period k is identified as

$$[\underline{f_i}(k)..\overline{f_i}(k)] = [U_i(t_{k-1})..U_i(t_k)], \tag{8}$$

where $\underline{f_i}(k)$ and $\overline{f_i}(k)$ represent the cumulative flow levels corresponding to the first and last vehicle that departed during period k respectively. Note that this range excludes traffic $Q_i(t_{k-1})$ as it departed during the previous period but was held up in a vertical queue on the considered link i itself.

The second type are links that are used by at least one route that was affected by active bottleneck(s) upstream (i.e. links that were (also) used by paths for which $\prod_{i'j' \in IJ_{p,i}} \alpha_{i'}(k) < 1$). Illustrated in Figure 7, for these links, demand that was held up during the previous time period in bottlenecks upstream ($\bar{Q}_i(t_{k-1})$) is deducted, while the demand that was held up during the current time period in bottlenecks upstream ($\bar{Q}_i(t_k)$) is added to the range of cumulative flow that has departed in the considered time period, thus defining the relevant cumulative flow levels as:

$$[\underline{f_i}(k)..\overline{f_i}(k)] = [U_i(t_{k-1}) + \bar{Q}_i(t_{k-1})..U_i(t_k) + \bar{Q}_i(t_k)]. \tag{9}$$

Note that $\underline{f_i}(k+1) = \overline{f_i}(k)$, hence in each time period, only $\overline{f_i}(k)$ needs to be computed.

The amount of demand held up in upstream bottleneck(s) is derived by summing residual traffic from queues on upstream turns $i'j'$ on routes that use link i using:

$$\bar{Q}_i(t_k) = \sum_{p \in P_i} \sum_{i'j' \in IJ_{p,i}} Q_{i'j',s_p}(t_k), \tag{10}$$

where P_i is the set of routes using the considered link i and s_p the destination of route p. Alternatively, $\bar{Q}_i(t_k)$ can also be derived on link level by deducting the link inflow from the

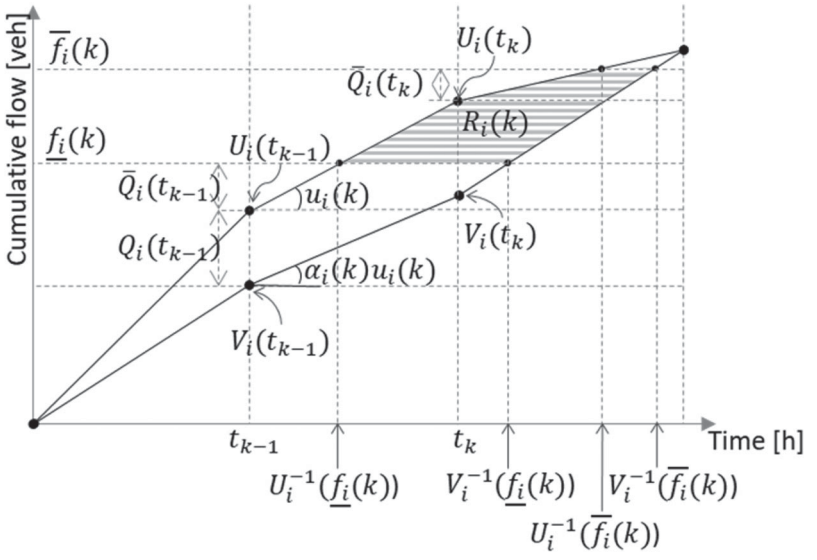

Figure 7. Example of collective loss calculation from a traveller's perspective on a link where at least one route was affected by upstream bottleneck(s) during periods *k* - 1 and *k*.

link demand:

$$\bar{Q}_i(t_k) = \sum_{p \in P_i} \pi_{p,rs}(k) D_{rs}(k) - u_i(k)(t_k - t_{k-1}). \tag{11}$$

One might argue that, when $\bar{Q}_i(\cdot)$ partly consists of residual traffic that was held up in an upstream bottleneck in the current time period after it was transferred from a bottleneck even further upstream from a previous time period, range (9) would not be continuous. However, it is assumed that it is, in order to avoid bookkeeping of transferred demand (subsection 3.2), thereby maintaining computational efficiency and simplicity.

3.4.2.2. Determination of the set of relevant points in time. As illustrated in Figure 7, the inverse functions of Equation (4) are used to determine the entry and exit times of the first vehicle as $U_i^{-1}(\underline{f_i}(k))$ and $V_i^{-1}(\underline{f_i}(k))$ respectively, and the entry and exit times of the last vehicle as $U_i^{-1}(\overline{f_i}(k))$ and $V_i^{-1}(\overline{f_i}(k))$ respectively, together forming the set of entry/exit times:

$$\mathcal{F}_i = \{U_i^{-1}(\underline{f_i}(k)), V_i^{-1}(\underline{f_i}(k)), U_i^{-1}(\overline{f_i}(k)), V_i^{-1}(\overline{f_i}(k))\}. \tag{12}$$

From the set of all start times $\mathcal{T} = \{0, t_1, .., t_{|K|-1}\}$, the start times that lie between the first entry and last exit time are added such that the set of relevant points in time is defined as:

$$\mathcal{G}_i = \mathcal{F}_i + \{t \in \mathcal{T} : U_i^{-1}(\underline{f_i}(k)) < t < V_i^{-1}(\overline{f_i}(k))\}. \tag{13}$$

After ordering from low to high, elements in $\mathcal{G}_i$ are referred to as t_n with $n = 1..|\mathcal{G}|$.

3.4.2.3. Calculation of collective loss and average delay per departure time period. The points in time in $\mathcal{G}$ together with the associated cumulative flow levels describe the vertices

of the triangles and quadrilaterals that, when summed, form the total surface representing the collective loss for traffic departed in a considered time period k:

$$R_i(k) = \sum_{n \in 1..|\mathcal{G}|} r_i(k, t_n), \tag{14}$$

with

$$r_i(k, t_n) = \frac{(t_n - t_{n-1})(\overline{U_i}(k, t_{n-1}) - \underline{V_i}(k, t_{n-1}) + \overline{U_i}(k, t_n) - \underline{V_i}(k, t_n))}{2} \tag{15}$$

and

$$\begin{aligned} \overline{U_i}(k, t_n) &= \min[U_i(t_n), \overline{f_i}(k)] \\ \underline{V_i}(k, t_n) &= \max[V_i(t_n), \underline{f_i}(k)] \end{aligned} \tag{16}$$

Note that Equation (15) is a special form of Equation (5) that restricts the surface to within cumulative flow levels of the first and last vehicle departed in the considered time period.

Finally, the average delay is derived by dividing collective loss by the number of vehicles using the link during period k:

$$\tau_i(k) = \frac{R_i(k)}{\overline{f_i}(k) - \underline{f_i}(k)} \tag{17}$$

where $\tau_i(k)$ represents the average delay per vehicle on link i that departed during period k.

The network-wide collective loss from the traveller's perspective for traffic departed in period k ($R(k)$) is derived by taking the sum of collective losses per link per departure time from Equation (14):

$$R(k) = \sum_i R_i(k) \tag{18}$$

3.4.3. Traveller's perspective – route level (for use in user equilibrium algorithms)

On the route level, the most important application type for the traveller's perspective is the evaluation of route delays within iterative solution algorithms imposing equilibrium conditions. This application type requires that the route delays are calculated using only information from the previous and current time period, as information for the next time period is dependent on the solution for the current time period and thus not available.

This means that, in contrast to the calculation of delay on link level from the traveller's perspective (subsection 3.4.2), the conditions of the next time period are not taken into account, as they are unknown. This is consistent with the definition of our semi-dynamic TA model in which only residual traffic is transferred to the next time period (subsection 2.1) and the definition of semi-dynamic TA models in general (Bliemer et al. 2017). Also, as most travellers use information from route-planners that provide current instead of expected future route-delays, it probably leads to more realistic choice behaviour.

The travel time on a route experienced by the traveller is equal to the summation of travel times on all links in the route, where for each link, the travel time at the time of entering the link is used. Hence, a trajectory through space (the links in the route) and time must be used to determine the travel time, given a specific departure time.

The instantaneous forward flow propagation assumption (subsection 2.1) in the static capacity-constrained TA model causes demand on a route without upstream bottlenecks to arrive earlier at a specific link (i.e. instantaneously) than demand on a route that experiences delay from some upstream bottleneck, whereas, as illustrated in the left part of Figure 5, the stationary travel demand assumption causes queues to be non-stationary, but growing (Bliemer et al. 2014; Gentile, Velonà, and Cantarella 2015).

The combination of these two assumptions cause demand on a route without upstream bottlenecks to experience less delay on a specific link than demand on a route that experiences delay on some upstream bottleneck, which means that the delay on some bottleneck link i (i.e. $\alpha_i(k) < 1$) varies for different routes using the link, depending on the delay that was experienced in upstream bottleneck links. In other words, route queuing delays are non-separable over links whenever there is more than one bottleneck on the route. This was recognised in Bliemer et al. (2014), who derived the following expression for the average route queuing delays on route p using only information from period k:

$$\dot{\tau}_{p,i}(k) = \frac{t_k - t_{k-1}}{2}\left(\frac{1}{\prod_{ij \in IJ_{p,i}} \alpha_i(k)} - 1\right). \tag{19}$$

3.4.4. Traveller's perspective – route level (for use in e.g. departure time choice models)

For application types in which information from time periods after the current time period can be used, more accurate (semi-dynamic) route delays can be derived. Typical application types would be the application of a departure time choice model based on travel times fed back from the semi-dynamic TA model and travel demand matrix estimation procedures that simultaneously handle multiple time periods.

For such application types, queuing delays on route p up to link i may be calculated by creating trajectories through (discretised) space and time, i.e.:

$$\tau_{p,i}(k) = \sum_{i'j' \in IJ_{p,i}} \tau_{i'}(k) \tag{20}$$

where $\tau_i(k)$ the delay on link i in period k calculated using Equation (17). Note that although it allows to include information from time periods after the current time period, this approach ignores the non-separability of route queuing delays (discussed in 3.4.3), just as van der Gun, Pel, and van Arem (2020) do. Section 5.2 further discusses the implications that this inconsistency has on the application range.

Further note that, conceptually, Equation (20) is in line with the approach to determine the amount of residual traffic adopted by the models in the first two rows of Table 1: comparing the total travel time to the duration of relevant time periods, assuming stationary travel demand (i.e. a uniform distribution of departure times within each time period). However, Equation (20) accounts for queues from the presented semi-dynamic capacity-constrained TA model, whereas the other approach does not account for queues.

4. Applications

To give insights into the accuracy and stability of the proposed semi-dynamic TA model compared to its static and dynamic counterparts, this section compares its outcomes

Table 3. Differences between the dynamic, semi-dynamic, and static TA models compared in this section.

	Temporal interaction assumptions		Spatial interaction assumptions			
			Wave speeds			
Publication	Travel demand	Traffic transfer	Hypo-Critical	Hyper-Critical	Fundamental diagram	Constraints
Bliemer and Raadsen 2018	Dynamic	All residual traffic	Kinematic	Kinematic	Concave-linear	Capacity + storage
This paper	Semi-Dynamic	Queues only	Infinite	Zero	Concave-flat	Capacity only
Bliemer et al 2014, Brederode et al 2019	Static	None	Infinite	Zero	Concave-flat	Capacity only

on two theoretical model instances (subsections 4.1 and 4.2) with those from the static capacity-constrained TA model from subsection 3.1 (Bliemer et al. 2014) and the dynamic TA model described in Bliemer and Raadsen (2018). Furthermore, to give insights into the scalability and the effect of the empty network assumption, subsection 4.3 repeats the comparison with the static TA model for a third, real-scale model instance. Because the dynamic TA model is not able to converge to SUE conditions a comparison with it is omitted for this model instance.

Because the focus of the comparisons in this section is on differences in the TA models and not their inputs, the travel demand defined for the semi-dynamic model instances is also used as input to the static and dynamic TA model instances. For the static TA model instances this means that a sequence of static assignments (one for each period defined in the semi-dynamic travel demand) is run, whereas for the dynamic TA model instances this means that demand is kept stationary and during (relatively large) semi-dynamic time periods. The effect of this choice is that differences between the three types of models in this section are smaller than they typically will be in real-world transport model applications, as these use a single (and larger) time period for static and more (and smaller) time periods for dynamic TA models.

The specific static and dynamic TA models are selected for comparison, as these are the closest related TA models that run on real-scale transport model systems. This is illustrated in Table 3, which lists only the properties (using the definitions from Bliemer et al. (2017)) for which the models differ. The differences with respect to the travel demand and traffic transfer relate to the temporal interaction assumptions whereas the other differences relate to the spatial interaction assumptions from Figure 1. Note that the differences with respect to the fundamental diagram and the constraints (last two columns) are considered a result of the assumption with respect to the hypercritical wave speed. Because the static and semi-dynamic TA models assume a zero hypercritical wave speed, vertical queues are assumed, which means that: (1) the hypercritical branch of the FD becomes flat (as displayed in the left part of Figure 4), and (2) there cannot be storage constraints. This means that only three assumptions in Table 3 (travel demand, traffic transfer, and hypercritical wave speeds) are the true drivers of all differences.

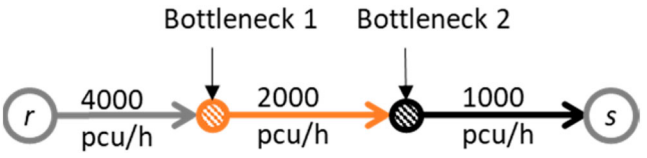

Figure 8. Link capacities of the corridor network with two bottlenecks.

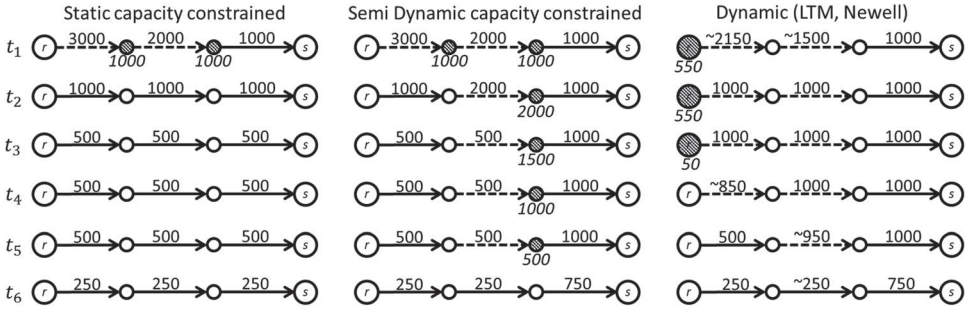

Figure 9. Link flows [pcu/h] (regular font) and vertical queues [pcu∗h] (italics below shaded nodes) per time period from the three TA models. Links conditions are indicated by continuous (uncongested) and dashed (congested) arrows.

4.1. Evaluating accuracy: corridor network with two bottlenecks

The corridor network with two bottlenecks was constructed to demonstrate differences in accuracy (of traffic conditions and collective losses) from the network operator's perspective in a situation where both flow reduction downstream and spillback upstream occur. Figure 8 displays the link capacities in person car equivalents per hour (pcu/h), whereas the top left graph of Figure 10 displays the travel demands for each of the seven defined one-hour time periods. Link lengths are 1 km for all three links. The semi-dynamic and dynamic TA models use free-flow speeds of 120 km/h and (to simplify the examples) a triangular (instead of QL) fundamental diagram. For the dynamic TA model, jam density is set to 180pcu/km for each lane of 2000 pcu/h. Note that these inputs imply initial queues of 1000 pcu/h in front of the second and third links.

Figure 9 summarises link flows, conditions, and vertical queues per time period as calculated by each of the three different TA models. Italics indicate the size of vertical queues at the end of the time period, dashed lines indicate congested links. In the dynamic TA model results, time-averaged flows are reported, and values starting with a tilde are rounded to the nearest 50 pcu/h. The upper right and bottom graphs in Figure 10 display the corresponding cumulative collective losses from the network operator's perspective. The cumulative collective loss (on link or network level) is the summation of collective losses from the start of the simulation up to and including the considered time period.

These figures indicate that in the static TA model, the total collective loss amounts 2000 pcu-hours occurring only in $\{t_1, t_2\}$, and only due to queues that had built up in t_1 and shrink in t_2, whereas in the semi-dynamic and dynamic TA models, total collective loss amounts to some 7000 pcu-hours occurring in $\{t_1..t_5\}$ for both models. Furthermore, in the static and semi-dynamic TA models, there is no spillback, whereas in the dynamic TA model, $\{t_1..t_5\}$

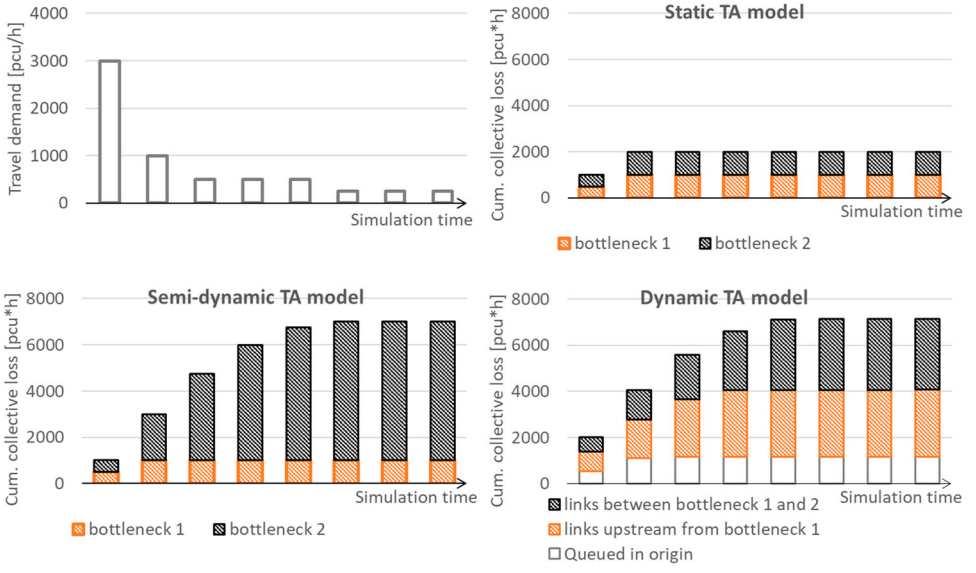

Figure 10. Travel demand (top left) and corresponding cumulative collective vehicle losses from network operator's perspective per time period for the static (top right), semi-dynamic (bottom left) and dynamic (bottom right) TA models.

the queue from the second bottleneck spills back onto the first bottleneck location whilst during $\{t_1..t_3\}$ the queue spills back further onto the origin, where it is modelled as a vertical queue.

This comparison shows that the size and temporal distribution of queues and collective losses from the semi-dynamic and dynamic TA models are very similar, but the spatial distribution (i.e. the congestion pattern) is different as the semi-dynamic TA model ignores spillback. Furthermore, it shows that the static TA model does not resemble the other two TA models on size, the temporal or spatial distribution of queues, and collective losses.

4.1.1. Detailed comparison between static and semi-dynamic TA model outcomes

Considering the static and semi-dynamic TA model outcomes in t_1, the collective losses are 1000 pcu-hours for both models, comprised of 500 pcu-hours (the average of a new queue growing to 1000 pcu in one hour) on both bottlenecks. The indifference between static and semi-dynamic outcomes is due to the empty network assumption (subsection 2.1) which in t_1 automatically holds for both models.

Considering the static and semi-dynamic TA model outcomes in t_2, the static TA model 'forgets' about the residual traffic on the network, causing Equation (5) to only account for the collective loss due to the dissolving queues (500 pcu-hours for both bottlenecks), whereas in the semi-dynamic TA model, the residual traffic from t_1 (1000 pcu on both bottlenecks) and demand departed during t_2 causes a dissolved queue at the first bottleneck and a queue of 2000 pcu at the second bottleneck at the end of t_2. This effectively means that demand departed in t_2 equals the network outflow, i.e. the semi-dynamic outcomes include an additional stationary queue of 1000 pcu. In $\{t_3..t_6\}$, the static TA assumes no queues, whereas in the semi-dynamic TA, the remaining queue shrinks until it has dissolved

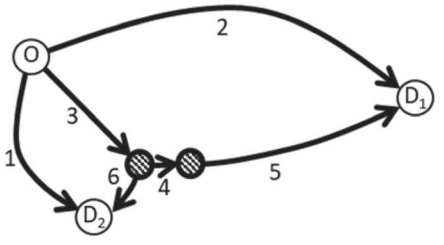

Link #	Length [km]	Free speed [km/h]	Capacity [veh/h]
1	5	100	2000
2	10	100	2000
3	4	120	4000
4	0.5	120	2000
5	5.5	120	1000
6	1	120	1500

Figure 11. Theoretical network (links 4, 5, and 6 are active bottlenecks in SUE conditions).

Table 4. Semi-dynamic Od demands for the network with two congested OD-pairs sharing a bottleneck.

OD-pair	t_1	t_2	t_3
$O - D_1$	1750	2000	1750
$O - D_2$	2750	3000	2750

at the end of t_6, at which time the difference between static and semi-dynamic cumulative collective losses has risen to 5000 pcu-hours.

4.1.2. Detailed comparison between semi-dynamic and dynamic TA model outcomes

Considering the semi-dynamic and dynamic TA model outcomes, given the equal model inputs, all differences are related to spillback. Once the queue from the second bottleneck spills back, the effective capacity of the upstream links is reduced to 1000 pcu/h, whereas in the semi-dynamic model, they remain at their original values throughout the simulation. As inputs of the dynamic TA model imply a backward wave speed of $\sim$12 km/h, spillback onto the first bottleneck occurs in t_1 after $\sim$5 min, whereas spillback onto the origin occurs in t_1 after 15 min. Because traffic is confronted with a reduced capacity further upstream, losses during t_1 are twice as high in the dynamic TA model. During t_2 however, the collective losses are practically equal, as for this time period, the residual demands from the previous time period in the semi-dynamic TA model are equal to the queues stored on the upstream links in the dynamic TA model, while in both models only bottleneck 2 is active. Although spatially distributed differently, total collective losses during $\{t_3..t_6\}$ are practically equal.

4.2. Evaluating stability: two congested OD pairs sharing a bottleneck

To demonstrate the stability (i.e. the extent to which stochastic user equilibrium conditions are attained), the theoretical network displayed in Figure 11 is selected from Brederode et al. (2016). The static demand for this network was extended to the semi-dynamic demand for three time periods as displayed in Table 4.

This network is hard to equilibrate for two reasons. Firstly, route costs on this network are strongly inseparable due to a shared active bottleneck at the downstream node of link 3 and due to spillback from the second bottleneck (at the downstream node of link 4) towards the origin. Secondly, the network is very sensitive, because travel demand, link capacities, and free flow speeds are chosen in a way that in SUE conditions, the (vertical) queues on the network are very small (Table 5). This means that bottlenecks may (de-)activate from only

Table 5. Sizes of vertical queues [pcu] in static and semi-dynamic TA models in SUE conditions.

	Queue on link 3			Queue on link4		
	t_1	t_2	t_3	t_1	t_2	t_3
Static	10.39	15.61	10.39	0.00	0.14	0.00
Semi-dynamic	10.39	15.74	10.60	0.00	0.18	0.00
Difference	0.00	0.13	0.21	0.00	0.04	0.00

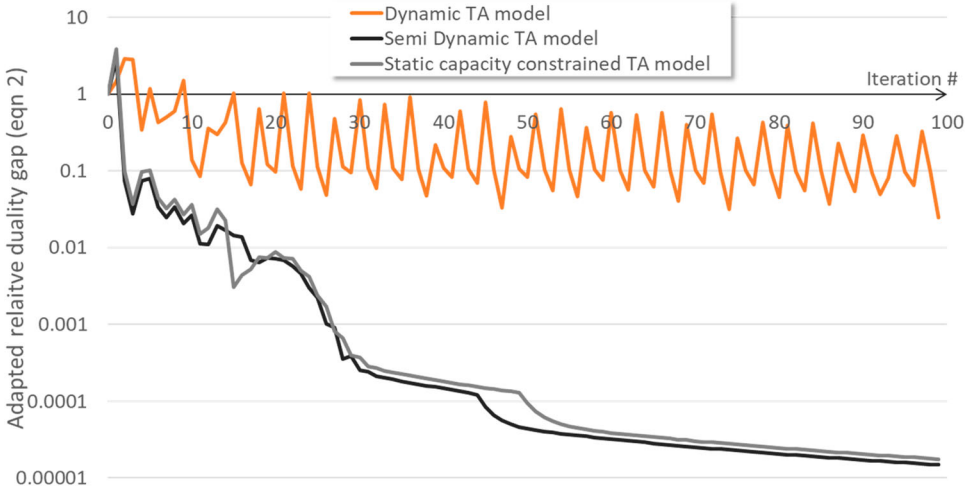

Figure 12. Adapted relative duality gap per iteration for the three TA models demonstrating that only static and semi-dynamic TA model converge on the considered test network.

small changes in route choice probabilities that occur during equilibration causing sudden changes in route costs.

All three TA models were run for 100 iterations using the settings described in 4.1 and the method of successive averages to equally average route fractions over iterations. Furthermore, in the dynamic TA model, route choice moments at the start of each time period are applied, to align it with the route choice moments in the static and semi-dynamic TA models. Figure 12 displays the adapted relative duality gap (Equation (2)) per iteration for each of the three tested TA models. This figure indicates that the semi-dynamic TA model maintains the stability conditions from the static TA model (reaching the required 1E-04 threshold after about 45–50 iterations), whereas they are not met by the dynamic TA model (as it does not reach values below 1E-02).

The convergence graphs of the static and semi-dynamic TA models are very similar. This is due to the relatively small vertical queues in SUE conditions (Table 5), which means that the amount of residual traffic and hence the difference between the static TA model (which ignores it) and the semi-dynamic TA model (which transfers it) is also very small.

The oscillations visible in the first 20–30 iterations in the static and semi-dynamic TA model are caused by the averaging scheme overshooting and thereby temporarily de-activating bottleneck(s) and thus become inconsistent with the network state under SUE conditions. This mechanism was recognised in Brederode et al. (2016), which referred to it as

the 'unstable phase'. After this phase, the correct network state is maintained smoothening convergence.

Closely related to this, note that although the semi-dynamic TA model assigns slightly more demand, its convergence is slightly better than its static counterpart. This is because the additional demand increases the size of the vertical queues (last row in Table 5) and therefore causes the network state in SUE conditions ('the stable phase') to be attained in less iterations. This specific network shows that a more congested network does not always correspond to a less stable network, although in most cases (and hence in real-scale transport networks) this will be the case, as illustrated by the applications in (Brederode et al. 2019). In general, it is expected that on real-scale transport networks, convergence of the semi-dynamic TA model is expected to be slightly worse compared to the static TA model.

4.3. Evaluating scalability and the effect of the empty network assumption on a real-scale network

To give insights into the scalability of the semi-dynamic TA model, but also in the order of magnitude of the effect of relaxing the empty network assumption (subsection 2.1) on outcomes in a realistic transport model context, the static and semi-dynamic TA models were applied on the large-scale strategic transport model of the province of Noord-Brabant (abbreviated in Dutch to 'BBMB'). The study area of this model is home to some 2.5 million residents and includes large urban areas in the form of the cities of Eindhoven, Tilburg, Breda, and Den Bosch. The network and prior OD demand for road traffic of the base year (2015, version S107) of the BBMB were used. This network contains 1425 centroids, $\sim$145000 links, and $\sim$103000 nodes.

Trip-purpose specific OD matrices (including freight) from the BBMB describing demand on an average workday were split up into 24 time periods of 1 h using purpose specific split factors and then summed up over trip purposes. Within these matrices, 1.590.247 OD pairs with nonzero demand in one or more time periods existed. During assignment 4.019.425 unique routes were generated and used, yielding 2.52 routes per OD pair on average. For illustrative purposes, Figure 13 displays assignment results for the busiest time period (08:00–09:00).

4.3.1. Scalability

The static and semi-dynamic TA models were both run for each of the 24 time periods until equilibrium using a threshold value of 1E-04 on the duality gap (Equation (2)). As there are no queues in the semi-dynamic TA model on the BBMB network before 6:00 and after 20:00; the empty network assumption holds for both TA models during these periods. This means that results and calculation times for these periods are the same. Therefore, these time periods are left from the analysis below.

Figure 14 displays calculation times per time period for both TA models. The numbers above the bars for assignment indicate the number of iterations required to reach user equilibrium conditions in the considered time period. Both TA models were run on a machine with AMD Ryzen 9 3900X CPU (12 cores) @3.79 Ghz and 128GB of RAM. Calculation times per time period in the static TA model vary between 1:08 h and 1:30 h requiring 8 up to 11 iterations, whereas the semi-dynamic TA model requires up to 1:44 h (+16%) and 13 iterations (+18%) for the assignments themselves. On top of that, the transfer of residual traffic

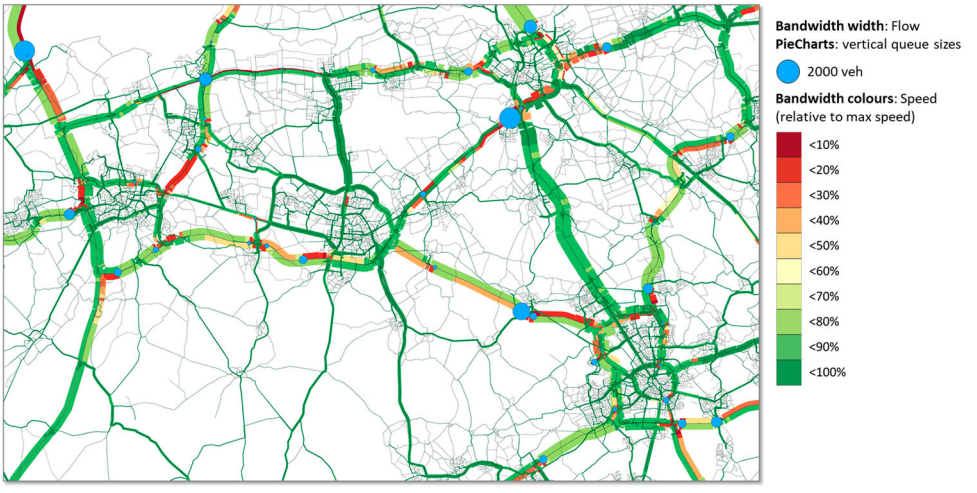

Figure 13. Assignment results for the study area of the BBMB model during its busiest time period (08:00–09:00).

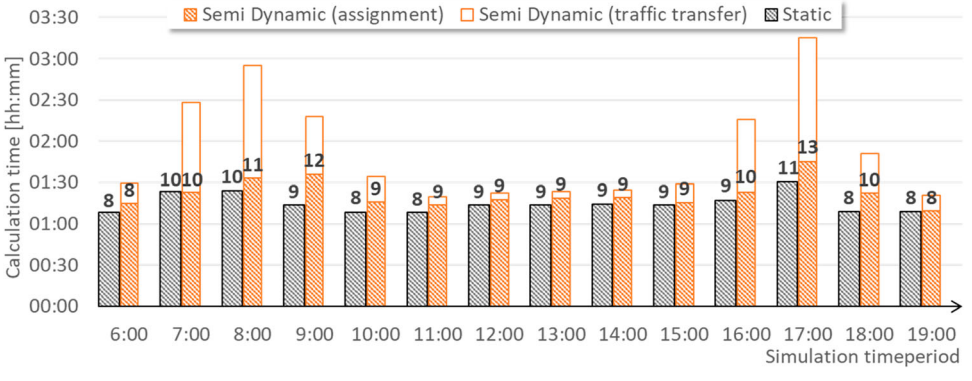

Figure 14. Calculation times (bars) and #iterations (numbers) per time period for static and semi-dynamic TA models on BBMB demonstrate that the traffic transfer causes most of the additional calculation time.

within the semi-dynamic TA model requires an additional 5 min up to 1:30 h (so up to +50% compared to the static TA model).

Table 6 compares (time) averaged and total calculation times. This shows that in time periods with queues, the semi-dynamic TA model requires on average 51% more calculation time, predominantly due to calculation time spent by the traffic transfer module. It should be noted however that the assignment model implementation is optimised C++ code, whereas the residual traffic transfer module is a prototypical implementation in Ruby using file-based data exchange with the assignment model. Given its low computational complexity, it is expected that the additional calculation time for the residual traffic transfer module could easily be reduced to less than 10% when its implementation would be merged with the assignment model code into a single code base.

Table 6. Comparison of minimum, maximum, average, and summed calculation times in [hh:mm].

	Static Assignment	Semi-dynamic			
		Assignment	Traffic transfer	Total	Difference
Average 6h-20h	01:14	01:21	00:31	01:53	51%
Total 6h-20h	17:27	19:06	07:19	26:26	51%
Total 24h	28:33	30:13	07:29	37:43	32%

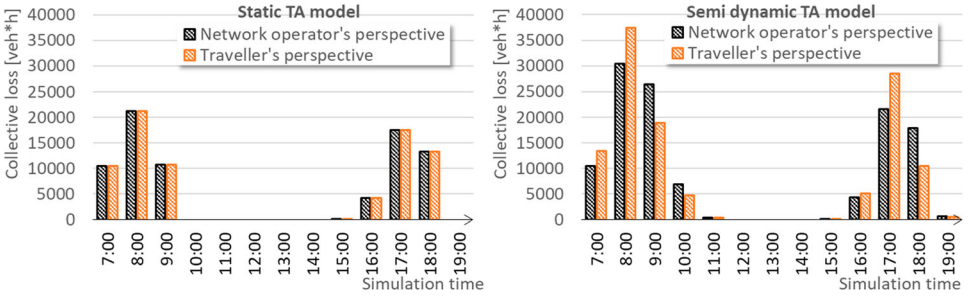

Figure 15. Network wide collective loss per hour from network operator's and traveller's perspective from static (left) and semi-dynamic (right) TA model application on Noord-Brabant model showing substantial collective loss increases and extension of peak periods.

Table 7. Collective losses from network operator's perspective and peak period durations from static and semi-dynamic TA model applications.

	Static TA model		Semi-dynamic TA model		Difference	
	Period	collective loss	Period	collective loss	absolute	relative
AM peak	07:00–10:00	42554	07:00–11:00	74774	32220	76%
PM peak	16:00–19:00	35156	16:00–19:00	44560	9404	27%
24 h period	00:00–24:00	77710	00:00–24:00	119334	41624	54%

4.3.2. Effect of the empty network assumption on collective loss and link flows

The black bars in Figure 15 and Table 7 compare the network-wide collective losses per hour from the network operator's perspective between the static and semi-dynamic TA models. This comparison shows that the relaxation of the empty network assumption by the semi-dynamic TA model yields more demand and hence more collective loss in time periods starting with residual traffic from a previous time period. On the BBMB, this yields up to 76% more collective losses during the peak periods and also the extension of especially the AM peak period. Considering the entire 24 h period, the semi-dynamic TA model yields 54% more collective loss. These substantial differences indicate that using a static TA model (i.e. assuming an empty network at the start of each assignment) severely under-estimates delays on congested networks. It is therefore very likely that the empty network assumption in static TA models influences (policy) decisions based on queue size and delay-related model outcomes on congested networks.

The orange bars in Figure 15 display the network-wide collective losses from traveller's perspective. Because the static TA model (left graph) omits residual traffic transfer, the cumulative flow corresponding to the first and last vehicles departed in a time period are equal to the cumulative in- and out-flow levels of that period (e.g. in Figure 7,

$\overline{f}_i(k) = U_i(t_k)$ and $\underline{f}_i(k) = V_i(t_{k-1})$), which causes the collective loss from the traveller's perspective (Equations (14)–(16)) to be equal to that from the network operator's perspective (Equation (5)).

Comparing collective losses from traveller's perspective with those from the network operator's perspective for the semi-dynamic TA model (right graph) demonstrates the difference between looking at when collective losses occur on the network versus looking at when travellers experiencing losses have departed. The surpluses of orange bars represent losses occurring later on the network, whereas surpluses of black bars represent losses occurring due to demand departed in earlier time periods.

5. Discussion

This section discusses properties and limitations specific to the semi-dynamic TA model. These in particular pertain to (potential) accuracy improvements with respect to handling and prioritisation of residual traffic (subsections 5.1 and 5.3), the definition of time period durations (subsection 5.4), and the route delay calculation method (subsection 5.2).

5.1. Omitting transfer of traffic based on total travel time

The accuracy of the approach in this paper could be further improved by not only transferring traffic held up in queues but also transferring traffic for which the calculated travel time is longer than the duration of the considered time period (following the approach from the models in the first two rows in Table 1). The authors deliberately choose to leave this topic for future research because (1) we see no means to integrate it into the TA model and hence it would require a post-processing step, and (2) it would introduce an optimisation problem around the equilibrium from the capacity constrained TA model. Both consequences would severely reduce tractability and stability whilst increasing computational requirements. Furthermore, in congested networks, including the effects of queuing is considered more important than including the effects of traffic not reaching its destination within a certain time period because (a) route choices are not affected, as these are still based on complete travel time, even if it exceeds the period duration; and (b) the proportion of trips with a longer duration than a typical time period duration in semi-dynamic TA models is relatively small.

5.2. Separable vs inseparable route delays

As mentioned in subsection 3.4.3, the flow propagation assumptions within the static capacity-constrained TA model yields route queuing delays that are non-separable over links (Bliemer et al. 2014). To remove non-separability, during route delay calculation (van der Gun, Pel, and van Arem 2020) (implicitly) assume instantaneous flow propagation for both congested and uncongested links. By doing so, the realism of individual route delays may increase, but this does introduce inconsistency between the route delay calculation (assuming instantaneous propagation, even when in a queue) and the TA model (assuming zero propagation when in a queue).

Because such an inconsistency reduces the stability and convergence properties of the model, we recommend to use the route delay calculation from subsection 3.4.3 (yielding

inseparable route delays) for any model application in which user equilibrium conditions are important. For model applications in which user equilibrium conditions are not important, the approach by van der Gun, Pel, and van Arem (2020) may be used to increase realism when comparing delays on individual OD pairs.

5.3. Influencing priority of transferred traffic

In this paper, for the sake of scalability and simplicity, residual traffic is transferred to a centroid connected to the upstream node of the link with the vertical queue as the origin (subsection 3.2), and, during the updating of cumulative flow curves, this is compensated for by subtraction of $Q_i(t_{k-1})$ in Equation (4). This means that transferred traffic from a previous time period has equal priority to demand from the current time period, and only higher priority to current demand that has encountered an upstream queue.

This subsection discusses an alternative method, in which the model user can steer the priority of transferred to current demand in situations where a queue remains in the current time period. In this method, residual traffic from a vertical queue in period k on node n_{ij} between links i and j is transferred into the OD matrix for period $k+1$ using an origin centroid that is directly connected to n_{ij}. This approach implicitly assumes that the queue discharge rate of the transferred demand instantly changes from $\alpha_{ij}(k)u_i(k)(t_{k+1} - t_k)$ into:

$$\frac{\alpha_{i'j}(k+1)\sum_{s\in S_{ij}} Q_{ij,s}(t_k)}{(t_{k+1} - t_k)}, \tag{21}$$

where i' represents the connector from the centroid storing the residual traffic to the node n_{ij} and S_{ij} is the set of destinations of the routes using turn ij in period k.

Now, the modeller can use the capacity of connector i' to influence to what extent the transferred traffic experiences delay traversing node n_{ij} in the next time period. When the capacity of the connector is set to a high value, $\alpha_{i'j}(k+1)$ approaches 1, hence the transferred traffic does not experience a queue while traversing node n_{ij}, whereas when it is set to a very low value, the same mechanism causes the transferred traffic to experience a very large queue while traversing node n_{ij}.

5.4. Transitions from queue discharge to departure rates

The method from subsection 5.3 allows to influence the priority of residual traffic only when the queue on n_{ij} persists in the next time period. But when the amount of (departed plus residual) traffic arriving at n_{ij} in the next time period is smaller than the normative capacity constraint on that node, $\alpha_{i'j}(k+1)$ equals 1, hence there is no queue and the transferred traffic does not experience a delay no matter what capacity is set for connector i'. Instead, in this case, the queue discharge rate instantly changes to a stationary 'departure' rate.

$$\frac{Q_{ij,s}(t_k)}{t_{k+1} - t_k}. \tag{22}$$

This demonstrates that the assumption of stationary travel demand within each time period in semi-dynamic TA model can result in residual traffic that 'departs' with a stationary departure rate depending on the duration of the next time period from the queue instead of with

the queue discharge rate from the previous time period. This effectively means that in the semi-dynamic TA model, the FiFo condition still holds within each time period, but may be violated across time periods.

This inconsistency is part of the very definition of the semi-dynamic TA model, and therefore cannot be removed. Instead, effects can only be reduced by shortening time periods. The optimal duration of the next time period should be a function of the discharge time of each queue according to the flow rates of the current time period. As the optimal duration is time period specific, such an approach will result in varying period durations within the semi-dynamic TA model. Note that only the discharge rate is considered relevant, because, for a shrinking queue, a too long duration causes it to prematurely dissolve, whereas for a growing queue, it only causes an instantaneous change in queue density.

6. Conclusions and recommendations

6.1. Findings and conclusions

This paper presents a straightforward extension of the static capacity-constrained TA model from Bliemer et al. (2014) and Brederode et al. (2019) into a semi-dynamic version. This effectively removes the empty network assumption, yielding a TA model that is more accurate than its static counterpart whilst, unlike its dynamic counterpart, it maintains the favourable stability and scalability properties required for application on large-scale strategic transport model systems. To the best of the authors knowledge, the presented approach is the only semi-dynamic TA model that places vertical queues at the correct location (on the upstream node of the link affected by capacity constraint(s)) whilst removing flow downstream from bottlenecks as part of the assignment model. The solution algorithm consists of the static TA model from Bliemer et al. (2014) and Brederode et al. (2019) set in a loop with a residual traffic transfer module. Collective losses and average delays on network, route, and link levels from the network operator's perspective (quantifying delay within a time period) and the traveller's perspective (quantifying delay within a *departure* time period) are determined from cumulative in- and out-flow curves as a post-processing module.

Outcomes from the semi-dynamic TA model were compared to its most closely related static (Bliemer et al. 2014; Brederode et al. 2019) and dynamic (Bliemer and Raadsen 2018) counterparts.

With respect to model accuracy, the comparison showed that the size and temporal distribution of queues and collective losses from the semi-dynamic and dynamic TA models are very similar, but the spatial distribution is different as the former model ignores spillback. Furthermore, it shows that the static TA model does not resemble the other two models on size, temporal, or spatial distribution of queues and collective losses.

Application of the static and semi-dynamic TA models on the large-scale strategic transport model of Noord-Brabant showed that the empty network assumption in the static TA model causes omission of 27% (PM peak) up to 76% (AM peak) of collective losses in busy periods and 54% when considering the 24 h period. It is therefore very likely that the empty network assumption in static TA models influences (policy) decisions based on queue size and delay-related model outcomes on congested networks.

With respect to model stability, the comparison showed that the semi-dynamic TA model maintains the stability from its static counterpart (reaching the required 1E-04 duality gap

threshold), whereas it is broken for the dynamic TA model (it does not reach the required duality gap threshold). This means that only the static and semi-dynamic TA models are suitable for strategic applications.

With respect to model scalability, the semi-dynamic TA model in its current (prototypical) form requires on average 51% more calculation time in time periods with queues, predominantly due to calculation time spent by the traffic transfer module. However, it is expected that the additional calculation time for the residual traffic transfer module could easily be reduced to less than 10% when its implementation would be merged with the assignment model code into a single code base. Authors argue that the additional calculation time is a worthwhile inconvenience to bear, given the substantial amount of collective loss being omitted by the static TA model due to its empty network assumption.

6.2. Recommendations

In this subsection, recommendations for further research are described, in order of priority from the authors' point of view.

With the shift from a static to a semi-dynamic TA model, the question arises how the study period time dimensions (the list of start- and end-time of each time period) should be defined. This could be done using an analytical approach that minimises e.g. the number of transitions from queue discharge to departure rate due to time period boundaries (subsection 5.4), or using a more empirical approach in which sensitivity analysis is conducted on the effect of different time dimensions on the model outcomes compared to observed data and/or outcomes of a dynamic TA model.

To determine the representativeness and robustness of the findings with respect to the effect of the empty network assumption (subsection 4.3.2), sensitivity analysis on the time dimensions (see previous paragraph) should be combined with a sensitivity analysis on the level of travel demand (what would happen if the temporal distribution of demand of the BBMB model would widen or narrow?) and ideally such analysis should be repeated on other realistic strategic transport models (especially with different levels of urbanisation and geographical density distributions).

As a follow up to the suggestion in subsections 3.2 and 5.3 to directly connect the residual traffic centroids to the queue location to be able to steer the priority of residual traffic, authors recommend to develop a method to automatically determine the values of the capacity of the connector links, such that the violation of FiFo across time periods is minimised.

Because the effects are expected to be negligible, but more importantly, to maintain good tractability, stability, and computational properties, the proposed semi-dynamic TA model o themits transfer of traffic for which the calculated travel time is longer than duration of the considered time period (subsection 5.1). To approximate the effect of this omission on model accuracy, the primary effect per time period could be determined by comparing the amount of traffic that would have been transferred based on total travel time (by post processing the outputs of the model application from 4.3) to the amount of traffic transferred by the proposed semi-dynamic TA model. Because the effects of the omission are larger for smaller time periods, this analysis could also lead to recommendations with respect to a lower bound value for time period durations in the semi-dynamic TA model.

One of the motivations to shift to a semi-dynamic TA model is that it is expected that especially departure time choice modelling and travel demand matrix estimation would greatly benefit from it (subsection 1.1). With respect to the prior, authors recommend to do research on how to embed it in a travel demand model containing a departure time choice model. With respect to the latter, the most straightforward way to continue would be to extend the matrix estimation method described in (Brederode et al. 2023) to an estimation period covering the whole day, allowing to include observed flows, delays, and congestion patterns on any temporal aggregation level. In line with the discussion from subsection 5.2, for both application types, a point of attention would be the effects of employing inseparable route delays in the TA model (Equation (19)) and separable route delays (Equation (20)) in the departure time choice model or matrix estimation method.

Notes

1. Some papers have deliberately been left out of this overview because they are either in Japanese (Akamatsu, Makino, and Takahashi 1998; Fujita, Yamamoto, and Matsui 1989; Fujita, Matsui, and Mizokami 1988; Kikuchi and Akamatsu 2007; Miyagi and Makimura 1991; Nakayama 2009) or they describe models merely as algorithms without a mathematical problem formulation (Davidson et al. 2011; Taylor 2003; Van Vliet 1982), which makes it hard to compare them to the model used in this paper.
2. By the definition from (Bliemer et al. 2017), some papers use the term quasi-dynamic instead.
3. For brevity, subscripts and arguments k are omitted for all variables in subsection 3.1 because within the static capacity constrained TA model, there are no relationships with other time periods.

Acknowledgements

The authors would like to thank the Dutch province of Noord-Brabant for providing the strategic transport model BBMB.

Disclosure statement

No potential conflict of interest was reported by the authors.

References

Akamatsu, Takashi, Yukio Makino, and Eikou Takahashi. 1998. "Semi-Dynamic Traffic Assignment Models with Queue Evolution and Elastic OD Demand." *Infrastructure Planning Review* 15: 535–545. https://doi.org/10.2208/journalip.15.535.

Bell, M. G. H., H. K. Lam, and Y. Lida. 1996. "A Time-Dependent Multi-Class Path Flow Estimator." Proceedings of the 13th International Symposium on Transportation and Traffic Theory, Lyon, France. https://trid.trb.org/view/481263.

Bliemer, Michiel, Mark Raadsen, Luuk Brederode, Michael Bell, Luc Wismans, and Mike Smith. 2017. "Genetics of Traffic Assignment Models for Strategic Transport Planning." *Transport Reviews* 37 (1): 56–78. doi:10.1080/01441647.2016.1207211.

Bliemer, Michiel, and Mark Raadsen. 2018. "Continuous-Time General Link Transmission Model with Simplified Fanning, Part I: Theory and Link Model Formulation." *Transportation Research Part B: Methodological* 126: 442–470. https://doi.org/10.1016/j.trb.2018.01.001.

Bliemer, Michiel, and Mark Raadsen. 2020. "Static Traffic Assignment with Residual Queues and Spillback." *Transportation Research Part B: Methodological* 132 (February): 303–319. https://doi.org/10.1016/j.trb.2019.02.010.

Bliemer, Michiel, Mark Raadsen, Erik De Romph, and Erik-Sander Smits. 2013. "Requirements for Traffic Assignment Models for Strategic Transport Planning: A Critical Assessment." Paper Presented at: Proceedings of the 36th Australasian Transport Research Forum 2013, ATRF, Brisbane, Australia, 2-4 October, 2013. Australasian Transport Research Forum. https://repository.tudelft.nl/islandora/object/uuid%3A7ab0d947-bf24-4d6e-bd1d-f85ae682398f.

Bliemer, Michiel, Mark Raadsen, Erik-Sander Smits, Bojian Zhou, and Michael Bell. 2014. "Quasi-Dynamic Traffic Assignment with Residual Point Queues Incorporating a First Order Node Model." *Transportation Research Part B: Methodological* 68 (October): 363–384. https://doi.org/10.1016/j.trb.2014.07.001.

Boyce, David, Biljana Ralevic-Dekic, and Hillel Bar-Gera. 2004. "Convergence of Traffic Assignments: How Much Is Enough?" *Journal of Transportation Engineering* 130 (1): 49–55. https://doi.org/10.1061/(ASCE)0733-947X(2004)130:1(49).

Brederode, Luuk, Martijn Heynicks, and Rogier Koopal. 2016. Quasi Dynamic Assignment on the Large Scale Congested Network of Noord-Brabant." In, 17. Barcelona: AET 2016 and contributors. https://www.researchgate.net/publication/309637604_Quasi_Dynamic_Assignment_on_the_Large_Scale_Congested_Network_of_Noord-Brabant.

Brederode, Luuk, Adam John Pel, Luc Wismans, and Erik de Romph. 2016. "Improving Convergence of Quasi Dynamic Assignment Models." Proceedings of the 6th International Symposium on Dynamic Traffic Assignment. https://research.tudelft.nl/files/56228843/DTA2016_extended_abstract_Improving_convergence_of_quasi_dynamic_assignment_models_revised.pdf.

Brederode, Luuk, Adam John Pel, Luc Wismans, Erik de Romph, and Serge Paul Hoogendoorn. 2019. "Static Traffic Assignment with Queuing: Model Properties and Applications." *Transportmetrica A: Transport Science* 15 (2): 179–214. https://doi.org/10.1080/23249935.2018.1453561.

Brederode, Luuk, Adam John Pel, Luc Wismans, Bernike Rijksen, and Serge Paul Hoogendoorn. 2023. "Travel Demand Matrix Estimation for Strategic Road Traffic Assignment Models with Strict Capacity Constraints and Residual Queues." *Transportation Research Part B: Methodological* 167 (January): 1–31. https://doi.org/10.1016/j.trb.2022.11.006.

Bui, Tien Thiem, Shoichiro Nakayama, Hiromichi Yamaguchi, and Kosuke Koike. 2019. "Link-Based Approach for Semi-Dynamic Stochastic User Equilibrium Traffic Assignment with Sensitivity Analysis Model." *Journal of Japan Society of Civil Engineers, Ser. D3 (Infrastructure Planning and Management)* 75 (5): I_615–I_625. https://doi.org/10.2208/jscejipm.75.I_615.

Caliper. 2010. "What Transcad Users Should Know About Traffic Assignment." https://pdfs.semanticscholar.org/b473/3cbdd5bf3d9cc216f34335c69c7e8e10baaf.pdf.

Canudas-de-Wit, C., and A. Ferrara. 2018. "A Variable-Length Cell Transmission Model for Road Traffic Systems." *Transportation Research Part C: Emerging Technologies* 97: 428–455. https://doi.org/10.1016/j.trc.2018.07.023.

Chan, Cy, Anu Kuncheria, Bingyu Zhao, Theophile Cabannes, Alexander Keimer, Bin Wang, Alexandre Bayen, and Jane Macfarlane. 2021. "Quasi-Dynamic Traffic Assignment Using High Performance Computing." *ArXiv:2104.12911 [Cs]*, May. http://arxiv.org/abs/2104.12911.

Daganzo, Carlos F. 1994. "The Cell Transmission Model: A Dynamic Representation of Highway Traffic Consistent with the Hydrodynamic Theory." *Transportation Research Part B: Methodological* 28 (4): 269–287. https://doi.org/10.1016/0191-2615(94)90002-7.

Daganzo, Carlos F. 1995. "The Cell Transmission Model, Part II: Network Traffic." *Transportation Research Part B: Methodological* 29 (2): 79–93. https://doi.org/10.1016/0191-2615(94)00022-R.

Davidson, Peter, Adam Thomas, Collins Teye-Ali, and Peter Davidson. 2011. "Clocktime Assignment: A New Mesoscopic Junction Delay Highway Assignment Approach to Continuously Assign Traffic Over the Whole Day," 12.

Fiorenzo-Catalano, M. S. 2007. "Choice Set Generation in Multi-Modal Transportation Networks." TRAIL. http://resolver.tudelft.nl/uuid:ef3b9c22-b979-4f46-9b02-110c82d67535.

Fisk, Caroline. 1980. "Some Developments in Equilibrium Traffic Assignment." *Transportation Research Part B: Methodological* 14 (3): 243–255. https://doi.org/10.1016/0191-2615(80)90004-1.

Flötteröd, Gunnar, and Stefan Flügel. 2015. "Traffic Assignment for Strategic Urban Transport Model Systems." In, 18. Oslo.

Friesz, Terry L., and Ke Han. 2019. "The Mathematical Foundations of Dynamic User Equilibrium." *Transportation Research Part B: Methodological* 126 (August): 309–328. https://doi.org/10.1016/j.trb.2018.08.015.

Fujita, Motohiro, Hiroshi Matsui, and Shoshi Mizokami. 1988. "Modelling of the Time-of-Day Traffic Assignment Over a Traffic Network." *Doboku Gakkai Ronbunshu* 389: 111–119. https://doi.org/10.2208/jscej.1988.111.

Fujita, Motohiro, Koshi Yamamoto, and Hiroshi Matsui. 1989. "Modelling of the Time-of-Day Traffic Assignment Over a Congested Network." *Doboku Gakkai Ronbunshu* 407: 129–138. https://doi.org/10.2208/jscej.1989.407_129.

Fusco, Gaetano, Chiara Colombaroni, and Stefano Lo Sardo. 2013. "A Quasi-Dynamic Traffic Assignment Model for Large Congested Urban Road Networks." *International Journal of Mathematical Models and Methods in Applied Sciences* 7 (May): 63–74.

Ge, Q., D. Fukuda, K. Han, and W. Song. 2020. "Reservoir-Based Surrogate Modeling of Dynamic User Equilibrium." *Transportation Research Part C: Emerging Technologies* 113: 350–369. https://doi.org/10.1016/j.trc.2019.10.010.

Gentile, Guido, Pietro Velonà, and Giulio Erberto Cantarella. 2015. "Uniqueness of Stochastic User Equilibrium with Asymmetric Volume-Delay Functions for Merging and Diversion." *EURO Journal on Transportation and Logistics* 3 (3): 309–331. https://doi.org/10.1007/s13676-013-0042-0.

Han, Ke, Terry L. Friesz, W. Y. Szeto, and Hongcheng Liu. 2015. "Elastic Demand Dynamic Network User Equilibrium: Formulation, Existence and Computation." *Transportation Research Part B: Methodological* 81 (Part 1 (November)): 183–209. https://doi.org/10.1016/j.trb.2015.07.008.

Himpe, Willem, Ruben Corthout, and Chris Tampère. 2016. "An Efficient Iterative Link Transmission Model." *Transportation Research Part B: Methodological, Within-day Dynamics in Transportation Networks* 92 (October): 170–190. https://doi.org/10.1016/j.trb.2015.12.013.

Himpe, Willem, R. Ginestou, and Chris Tampère. 2019. "High Performance Computing Applied to Dynamic Traffic Assignment." *Procedia Computer Science* 151: 409–416. https://doi.org/10.1016/j.procs.2019.04.056.

Kikuchi, S., and T. Akamatsu. 2007. "A Semi-Dynamic Traffic Equilibrium Assignment Model with Link Arrival and Departure Rates." *Journal of Infrastructure Planning and Management* 24: 577–585. https://doi.org/10.2208/journalip.24.577.

Koike, Kosuke, Shoichiro Nakayama, and Hiromichi Yamaguchi. 2022. "A Link-Based Semi-Dynamic User Equilibrium Traffic Assignment Model Considering Signal Effect." *Asian Transport Studies* 8 (January): 100062. https://doi.org/10.1016/j.eastsj.2022.100062.

Lam, William H. K., H. P. Lo, and Ning Zhang. 1996. "A Quasi-Dynamic Traffic Assignment Model with Time-Dependent Queues." *HKIE Transactions* 3 (2): 7–14. https://doi.org/10.1080/1023697X.1996.10667698.

Lam, William H. K., and Y. Zhang. 2000. "Capacity-Constrained Traffic Assignment in Networks with Residual Queues." *Journal of Transportation Engineering* 126 (2): 121–128. https://doi.org/10.1061/(ASCE)0733-947X(2000)126:2(121).

Liu, Henry X., Xiaozheng He, and Bingsheng He. 2007. "Method of Successive Weighted Averages (MSWA) and Self-Regulated Averaging Schemes for Solving Stochastic User Equilibrium Problem." *Networks and Spatial Economics* 9 (4): 485–503. https://doi.org/10.1007/s11067-007-9023-x.

Lo, Hong K., and W. Y. Szeto. 2002. "A Cell-Based Variational Inequality Formulation of the Dynamic User Optimal Assignment Problem." *Transportation Research Part B: Methodological* 36 (5): 421–443. https://doi.org/10.1016/S0191-2615(01)00011-X.

Miyagi, T., and K. Makimura. 1991. "A Study on Semi-Dynamic Traffic Assignment Method." *Traffic Engineering* 26: 17–28.

Nakayama, Shoichiro. 2009. "A Semi-Dynamic Assignment Model Considering Space-Time Movement of Traffic Congestion." *JSCE Journal of Infrastructure Planning & Management* 64 D: 340–353.

Nakayama, Shoichiro, and Richard Connors. 2014. "A Quasi-Dynamic Assignment Model That Guarantees Unique Network Equilibrium." *Transportmetrica A: Transport Science* 10 (7): 669–692. https://doi.org/10.1080/18128602.2012.751685.

Nakayama, Shoichiro, Jun-ichi Takayama, Junya Nakai, and Kazuki Nagao. 2012. "Semi-dynamic Traffic Assignment Model with Mode and Route Choices under Stochastic Travel Times." *Journal of Advanced Transportation* 46 (March): 269–281. https://doi.org/10.1002/atr.208.

Patil, Priyadarshan N., Katherine C. Ross, and Stephen D. Boyles. 2021. "Convergence Behavior for Traffic Assignment Characterization Metrics." *Transportmetrica A: Transport Science* 17 (4): 1244–1271. https://doi.org/10.1080/23249935.2020.1857883.

Petprakob, Wasuwat, Lalith Wijerathne, Takamasa Iryo, Junji Urata, Kazuki Fukuda, and Muneo Hori. 2018. "On the Implementation of High Performance Computing Extensionfor Day-to-Day Traffic Assignment." *Transportation Research Procedia* 34 (January): 267–274. https://doi.org/10.1016/j.trpro.2018.11.041.

Prato, Carlo Giacomo. 2009. "Route Choice Modeling: Past, Present and Future Research Directions." *Journal of Choice Modelling* 2 (1): 65–100. https://doi.org/10.1016/S1755-5345(13)70005-8.

Raadsen, Mark, and Michiel Bliemer. 2018. "General Solution Scheme for the Static Link Transmission Model." Sydney, Australia. https://ses.library.usyd.edu.au//bitstream/2123/19143/1/ITLS-WP-18-21.pdf.

Raadsen, Mark, and Michiel Bliemer. 2019. "Steady-State Link Travel Time Methods: Formulation, Derivation, Classification, and Unification." *Transportation Research Part B: Methodological* 122 (April): 167–191. https://doi.org/10.1016/j.trb.2019.01.014.

Simoni, M. D., and C. G. Claudel. 2020. "A Fast Lax–Hopf Algorithm to Solve the Lighthill–Whitham–Richards Traffic Flow Model on Networks." *Transportation Science* 54 (6): 1526–1534. https://doi.org/10.1287/trsc.2019.0951.

Smith, M. J. 2013. "A Link-Based Elastic Demand Equilibrium Model with Capacity Constraints and Queueing Delays." *Transportation Research Part C: Emerging Technologies* 29 (April): 131–147. https://doi.org/10.1016/j.trc.2012.04.011.

Smits, Erik-Sander, Adam John Pel, Michiel Bliemer, and Bart van Arem. 2018. "Generalized Multivariate Extreme Value Models for Explicit Route Choice Sets." *ArXiv:1808.04280 [Math, Stat]*, August. http://arxiv.org/abs/1808.04280.

Szeto, W. Y., and Hong K. Lo. 2006. "Dynamic Traffic Assignment: Properties and Extensions." *Transportmetrica* 2 (1): 31–52. https://doi.org/10.1080/18128600608685654.

Tampère, Chris M. J., Ruben Corthout, Dirk Cattrysse, and Lambertus H. Immers. 2011. "A Generic Class of First Order Node Models for Dynamic Macroscopic Simulation of Traffic Flows." *Transportation Research Part B: Methodological* 45 (1): 289–309. https://doi.org/10.1016/j.trb.2010.06.004.

Taylor, Nicholas. 2003. "The CONTRAM Dynamic Traffic Assignment Model." *Networks and Spatial Economics* 3 (October): 297–322. https://doi.org/10.1023/A:1025394201651.

van der Gun, Jeroen P. T., Adam J. Pel, and Bart van Arem. 2020. "Travel Times in Quasi-Dynamic Traffic Assignment." *Transportmetrica A: Transport Science* 16 (3): 865–891. https://doi.org/10.1080/23249935.2020.1720862.

Van Vliet, D. 1982. "Saturn – A Modern Assignment Model." *Traffic Engineering & Control* 23 (12), https://trid.trb.org/view/188929.

Wardrop, J. G. 1952. "Road Paper. Some Theoretical Aspects of Road Traffic Research." *Proceedings of the Institution of Civil Engineers* 1 (3): 325–362. https://doi.org/10.1680/ipeds.1952.11259.

Yperman, Isaak. 2007. "The Link Transmission Model for Dynamic Network Loading," 178.

Appendix

Appendix A: Definition of variables defined in section 3

For convenience of the reader, all indices, sets, constants, variables and vectors defined in section 3 are listed below:

Indices

k	Time period
r, s	Origin, destination

rs	OD-pair
p	Route
i	Link
ij	Turn from link i to link j

Sets

K	Time periods considered by the TA model
P_{rs}	Routes between r and s in some time period[3]
P_{ij}	Routes traversing turn from link i to link j in some time period[3]
RS	OD-Pairs with demand in some time period[3]
$IJ_{p,i}$	Turns on route p up to but excluding the turn from link i to link j
$\mathcal{F}_i$	Set of entry- and exit times of first and last vehicle on link i
$\mathcal{G}_i$	Set of relevant points in time for calculation of collected los on link I for traffic departed

Constants

μ_{rs}	Scale parameter describing the degree of travellers' perception errors on route travel times
t_k	End time of period k

Variables

$\pi_{p,rs}$	Route choice probability for route p on OD-pair rs in some time period[3]
c_p	Cost on route p in some time period[3]
ζ_{rs}	Minimum stochastic route cost on OD-pair rs in some time period[3]
α_{ij}	Flow acceptance factor on turn from inlink i to outlink j in some time period[3]
$Q_{ij,s}(t_k)$	Amount of residual traffic between turn ij and destination s at t_k
$\bar{Q}_i(t_k)$	Amount of residual traffic held up in bottlenecks upstream from link i during period k
$u_i(k)$	Inflow rate of link i during period k
$U_i(t_k)$	Cumulative inflow for link i at the end of period k
$V_i(t_k)$	Cumulative outflow for link i at the end of period k
$\tilde{R}_i(k)$	Collective loss on link i during period k
$R_i(k)$	Collective loss of vehicles using link i departed during k
$\tilde{R}(k)$	Network wide collective loss during period k
$R(k)$	Network wide collective loss for vehicles departed during period k
$\tilde{\tau}_i(k)$	Average delay per vehicle on link i during period k
$\tau_i(k)$	Average delay per vehicle departed during period k on link i
$\dot{\tau}_{p,i}(k)$	Average delay per vehicle departed during period k using route p upto link i (using only information upto and including time period k)
$\tau_{p,i}(k)$	Average delay per vehicle departed during period k using route p upto link i (using information from all time periods in K)
$\underline{f}_i(k), \overline{f}_i(k)$	Cumulative flow levels on link i corresponding to the first and last vehicle that departed during period k respectively

Vectors

$\mathbf{u}_k$	Inflows on all links in period k
$\mathbf{D}_k$	OD demands for all used OD pairs in period k
$\boldsymbol{\pi}_k$	Route choice probabilities for each route in the route set in period k
$\boldsymbol{P}$	All pre-generated routes used by the TA model in some time period[3]
$\boldsymbol{\alpha}_k$	Acceptance factors for links with vertical queue on its downstream node in period k
$\mathbf{Q}_k$	Residual traffic for all turning movement-destination combinations at t_k

Appendix B: Two derivations for determination of queue size at link level

The amount of traffic held up on the queue of a link *i* can be directly derived from the cumulative flow curves of the link by:

$$Q_i(t_k) = (1 - \alpha_i(k))u_i(k)(t_k - t_{k-1}) \tag{23}$$

or equivalently by summing residual traffic transferred from this link from Equation (3):

$$Q_i(t_k) = \sum_{j \in J_i} \sum_{s \in S_{ij}} Q_{ij,s}(k) \tag{24}$$

where J_i is the set of outlinks from link *i* and S_{ij} is the set of destinations for which in time period *k* residual traffic was transferred from a vertical queue on turn *ij*.